Investigation of High-Elevation Drivers of Snowpack and Streamflow Characteristics in the American West

By Ethan Heidtman[1, 2]
Advised by Dr. Karen Prestegaard[1]

[1]U. of Maryland, College Park, Department of Geology
[2]U. of Maryland, College Park, Department of Atmospheric & Oceanic Science

eheidtma@terpmail.umd.edu

Department of Geology Senior Thesis

GEOL394

April 23, 2024

Table of Contents

Table of Figures

Table of Tables

Abstract

Mountain snowpack is one of the most vital sources of freshwater for millions of people worldwide, and recent changes in snowpack depth and duration pose serious problems for people that depend on them for irrigation, drinking water, and other water needs. Significant snowpack decreases (>80%) have been observed in many locations throughout western North America over the last century, threatening an important water source: snowmelt. In this study I investigate the consequences of assuming a peak snowpack date of April 1 on snowpack trends from 1980 through 2022. Data from the Snow Telemetry Network (SNOTEL) for this time period at ~200 high-elevation locations and USGS mean daily discharge data from ~100 small watersheds were obtained. These data were used to compute snowpack magnitudes and timings, as well as their relationship to streamflow magnitudes and timings. Assuming that peak snowpack occurs on April 1 was found to play a more substantial role in masking true snowpack trends at higher elevations (> 2500 meters). At lower elevations, the April 1 assumption was less significant and external forces including rain and watershed morphology affected snowpack and snowmelt. At higher elevations, latitude rather than elevation affected the relationship between snowpack characteristics and the timing and magnitude of peak snowpack. Watershed area was found to have a notable influence on timing of snowmelt. This research indicates that the assumption of an April 1 date for maximum snowpack may not be valid, especially as snowpacks retreat to higher elevations with global warming. These results improve understanding of the latitude and basin area controls on the timing and magnitude of snowmelt events that is necessary to predict and improve water resource management and prediction in the American West, and worldwide.

Plain Text Abstract

Mountain snowpack is one of the most vital sources of water for millions of people around the world, as well as for Americans, particularly in the western United States. Temperature increases due to the emission of greenhouse gases and the resultant global warming has drastically impacted the extent of snowpack that develops each winter in many mountainous regions, including the Sierra Nevada and the Rockies. In many areas, snowpack has decreased by more than 80% over the last century. For those communities that depend on melting snow for drinking water, irrigation supply, and more, threats to snowpack are highly consequential. This work used daily snowpack and streamflow data collected at various different locations (121 and 69 sites, respectively) throughout the American West from 1980 through 2022 to explore the environmental conditions that drive these important snowpacks. An over-simplified assumption that many previous authors used in similar studies was challenged and found to be significantly influencing the current understanding of how snowpack is changing, particularly at high elevations. After narrowing the focus to even higher elevations, latitude and watershed size were found to play the most substantial role in the magnitude of snowpacks that developed and the timing of snowmelt from that snowpack in the spring. This work helped to identify the regions that will continue to be in need of water and what factors most readily control water availability for the people in those water-needy regions.

1.0 Introduction

Mountain snowpacks are a vital source of water in mountainous and mountain-adjacent regions worldwide, including the Himalaya and the Indian subcontinent, the Alps and their foothills, and the North American Cordillera and the surrounding plains. In recent years, water scarcity has been a highly publicized issue in the western United States, and elsewhere around the

globe. Research indicates that some western U.S. states obtain as much as 75% of their water supply from snowmelt; rivers that are fed almost entirely by snowmelt can shut off shortly after spring thaw when snowpacks are thin (Water Science School, 2019). Therefore, a weak snowpack season can require water usage restrictions from local and state governments in response to the water shortfalls. For example, the Colorado winter in 2001/2002 was abnormally dry and warm, resulting in snowpacks (as of the end of May 2002) that were less than 30% their long-term average (Kenney et al., 2004). As a result, streamflow was highly diminished in the summer of 2002 and the entire state of Colorado experienced extreme drought. It is estimated that around forty million people in the western United States are highly dependent on snowmelt for their drinking water and for irrigation, so situations similar to the Colorado summer of 2002 have serious consequences (University of Nevada, Reno, 2022).

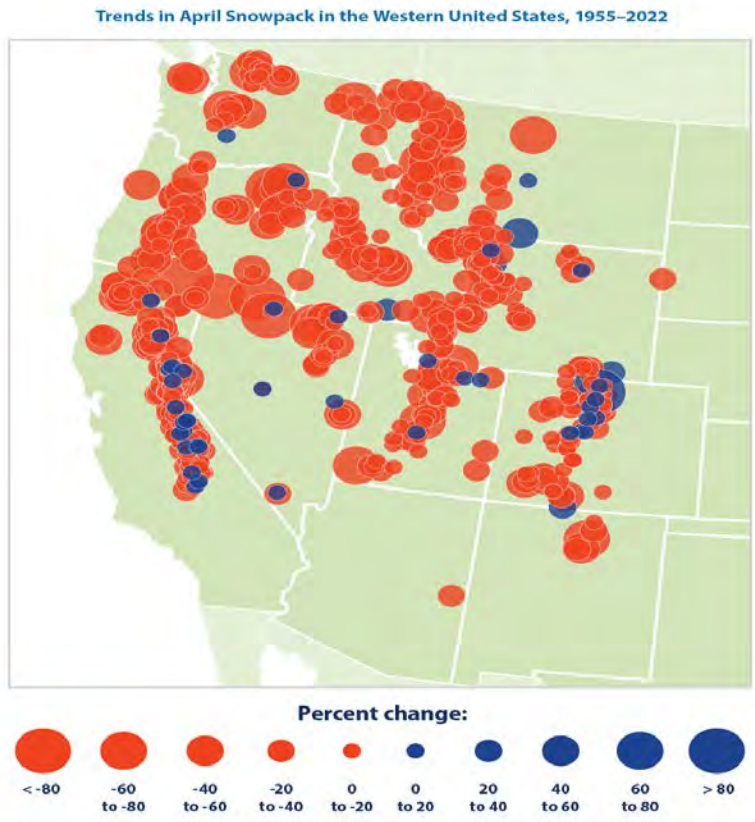

Figure 1 Trends in April 1 snowpack measured at SNOTEL stations from 1955 through 2022. Red locations represent % decreases in the extent of snowpack, blue dots represent increases. The size of the dot corresponds to the magnitude of the change. From U.S. EPA (2016).

The amount and timing of mountain snowmelt are dependent on many factors, including atmospheric conditions such as moisture content (humidity) and air temperature. Temperature is an important factor that affects both snow duration and snowpack thickness (McCabe et al., 2018). Temperature and snowpack are certainly not mutually exclusive or independent variables; water only freezes if the temperature is below 0ºC, and will not remain solid if the temperature ascends significantly past that threshold.

If temperature is one of the main drivers of snowpack development and melt, then increases in temperature as a result of global warming via the release of greenhouse gases will likely influence these mountain snowpacks in areas where it is a vital water supply, such as the American west (McCabe et al., 2018). **Figure 1** illustrates the significant changes that snowpacks have experienced over the last 67 years, from 1955-2022. In most mountain watersheds, snowpack has decreased in its magnitude and extent, with many locations seeing drops of 80% or more (U.S. EPA, 2016). Very few locations exhibited snowpack increases, and those that did were minor.

The timing and magnitude of snowmelt each year are dependent on many different factors, including air temperature and snowpack characteristics. Numerous studies have investigated how snowmelt timing has changed and will continue to change under past and future warming regimes

(Fang & Pomeroy, 2020; Dierauer et al., 2018). These studies often take similar approaches: separate baseflow from snowmelt, subtract baseflow out, and analyze the snowmelt component. Moreover, studies such as these that work with snowpack (snow water equivalent, for example) often make simplifying assumptions in the analysis of snowpack characteristics. A common assumption is that snowpack is assumed to reach its annual peak around April 1 (Miller & Piechota, 2011; Stewart et al., 2005; Clow, 2010).

The results in **Figure 1** were produced by the U.S. Environmental Protection Agency following the results from a group that published a number of papers utilizing the April 1 snowpack as a basis for their analyses (Mote et al., 2004 ; Mote, 2006; Mote et al., 2018). Each of these Mote papers states that using April 1 is a convention of the pre-automated measurement days. They find that April 1 "is the most frequent observation date" and that snow surveyors chose that date because on average the accumulation season ends on April 1 (Mote et al., 2018). The data collection methods used in these Mote studies, and others, were not automated extensively until 1980 at the earliest, and so April 1 may be valid for pre-1980 analyses. Moreover, this choice may have been valid during periods of stable climate, but as discussed above, snowpack patterns (quantified with the April 1 assumption) appear to be changing, and so it is feasible that the date of peak snowpack is changing too. The extent and magnitudes of snowpacks can exhibit inter-annual variations due to (1) underlying climate/weather variability and (2) long-term changes in climate. Therefore, April 1 may not always be a consistent rule-of-thumb for the date of maximum snowpack, and it may be a poor choice for studies of snowpack variation under conditions of climate change. Snowpack is often measured *in situ* as snow water equivalent (SWE), a measure of how much water is contained per volume of snow.

Many research groups use April 1 SWE as an approximator of available snowpack, and then link the snowpack to other processes, a choice that has consequences. Selection of April 1 SWE as the baseline for snowpack and snowmelt analyses result in underestimations of peak SWE, as well as large variance in the bias of these underestimations (Montoya et al., 2014). The same authors suggest that elevation is also a key factor in the bias associated with picking April 1 SWE. Consequently, elevation was be considered strongly in this work. Similarly, snow/rain ratios during the winter are widely decreasing in this region, particularly in the lower elevations (Knowles et al., 2006). These changing winter precipitation ratios are largely controlled by temperature and contribute to decreasing snowpacks.

Elevation plays a substantial role in snow deposition as well as melt dynamics, and so it would also impact mountain snowmelt flows come the melt season. One study found that elevation variability within mountain watersheds (which can span huge elevation ranges) results in variable melt characteristics, due to precipitation mixtures in particular (Hammond & Kampf, 2020). Slope aspect (the cardinal direction in which a slope faces) can also affect snowpack variability within watersheds, via variable shortwave solar radiative fluxes (López-Moreno et al., 2014). Additionally, rain-influenced catchments can see earlier streamflow peaks than in snow-dominated systems (due to rain-on-snow events), although the partitioning of streamflow (rain-driven vs. snow-driven flow) appears to be somewhat resistant to warming temperatures and climate change (Liu et al., 2013).

Basin morphology plays an important role in the melting of snowpack as well as the generation of streamflow. Basins can span thousands of meters of elevation, and there are consequently significant nuances that must be addressed to understand streamflow hydrology in mountainous regions. To address this, the current study examined the effect of basin size on snowpack and snowmelt runoff characteristics.

2.0 Research Objectives

The first goal of this study was to assess whether the assumption of using April 1 for peak snowpack generates significant errors in determining the timing and amount of peak snowpack, and subsequent errors in snowmelt calculations. The second goal of this study was to investigate whether basin location (latitude) and basin morphology (e.g., basin area) influence snowmelt and streamflow properties. The specific hypotheses are as follows:

Hypothesis 1: The selection of April 1 as the date of peak SWE imparts systematic underestimations of the magnitude of peak SWE, particularly at high-elevation sites.

Hypothesis 2: The selection of the April 1 date masks decadal or longer-term patterns in snowpack characteristics, particularly at high-elevation sites.

Hypothesis 3: Peak snowmelt discharge increases with basin area in northern latitude or high elevation watersheds, but may decrease or remain constant at lower latitudes and elevations.

Hypothesis 4: Time intervals between peak snowpack and peak snowmelt discharge increase with basin size.

Null Hypothesis (H1, H2): The April 1 assumption does not create systematic underestimations of peak snowpack and thus does not mask long-term trends in snowpack.

Null Hypothesis (H3, H4): Peak snowmelt discharge shows no relationship to basin area.

3.0 Data and Methods

Data for this study were obtained from two main data sources. Snow water equivalent (SWE) and air temperature data were collected by the United States Department of Agriculture via the Snow Telemetry Network (SNOTEL). Streamflow data was collected by the United States Geological Survey. These in-situ SWE data were accessed via a web interface, and the USGS streamflow data were collected in R by accessing an internet database through the United States Geological Survey. In order to test the hypotheses, R programming (Version 4.3.2) was utilized in the RStudio Environment (Version 2023.06.0+421) to collect, filter, and analyze the data (R Core Team, 2023). All visualizations not cited in-text were created in RStudio with R programming by myself and scripts are included in Section 11.3. Descriptions of the two datasets and methods for processing the data are described below.

3.1 Snow Water Equivalent and Air Temperature Data

This study utilizes the United States Department of Agriculture National Water and Climate Center's Snow Telemetry Network (SNOTEL) as the source of daily *in situ* data. Data from these remote monitoring stations were collected through the USDA Report Generator interface (https://wcc.sc.egov.usda.gov/reportGenerator/). The North American SNOTEL network provides daily measurements with recorded uncertainties for 897 individual locations, many of which are remote high-elevation clearings.

SWE and air temperature data were gathered from a daily record collected at all SNOTEL stations. SWE is a measure of how much liquid water is contained in a certain volume of snow. For SNOTEL, SWE is measured by a snow pillow and pressure transducer that measures the

weight of a given volume of snow on top of it, and turns that pressure into a density reading that can then be used to calculate the amount of water in the snow. Air temperature is measured by a shielded thermistor, a sensor that changes its electrical resistance with temperature. The SWE and air temperature data have recorded uncertainties of ± 0.1 inches (2.54 mm) and ± 0.1 ºC respectively (see the Appendix for an image of a SNOTEL station).

Data were collected from the existing record at all 897 SNOTEL stations over the period October 1, 1979 through September 30, 2022. SWE and air temperature were collected separately, and then compiled into two individual datasets via an R script written by hand. This current study was focused on only the contiguous United States, so Alaskan SNOTEL stations were filtered out. More data filtering was performed to ensure that both the SWE and temperature datasets had the same number of stations, and the same stations.

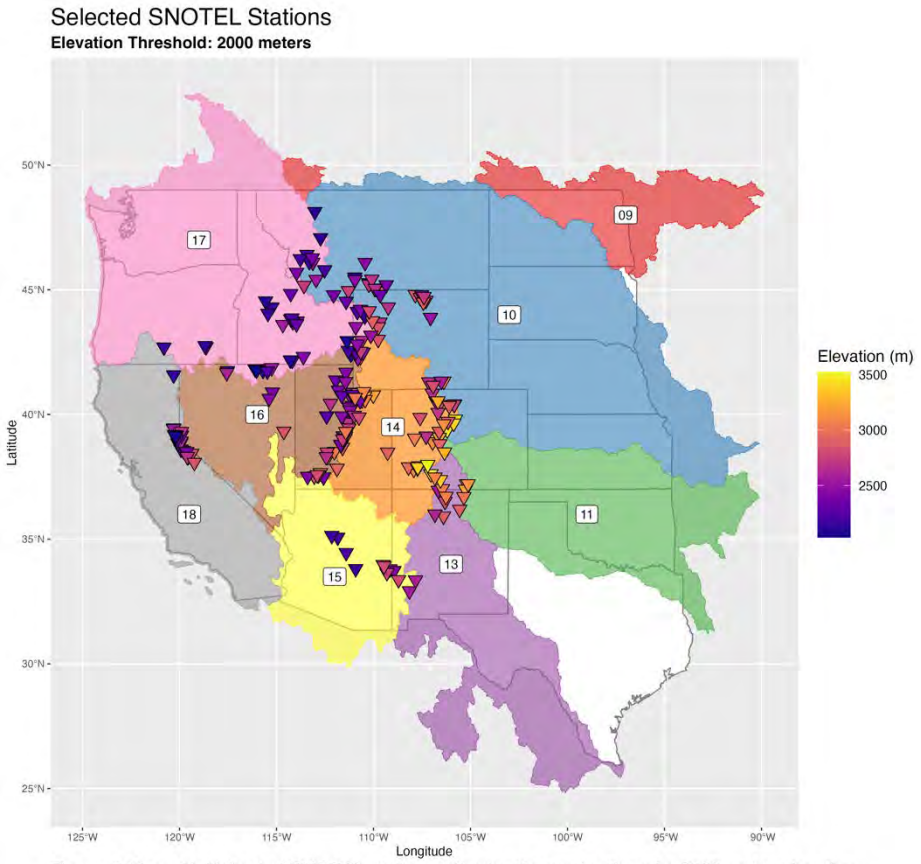

Figure 2 Map of initial set of SNOTEL stations following the application of a 2000-meter elevation filter. Total number of stations is 207, colored by elevation. Shaded regions are large river basins (HUC2s) that are numbered here.

Two consecutive elevation thresholds were used at different points of this work. Firstly, a threshold of 2000 meters, selecting only those SNOTEL stations above that line. The goal of this threshold was to limit outside influences on snow and watershed dynamics that may play more of a role near human population centers and the Pacific Coast. For example, the coastal region is more susceptible to intense seasonal rainfall, particularly in the Pacific Northwest. Teleconnections such as the El Niño Southern Oscillation (ENSO) can modify characteristics of precipitation variably in each of its phases (Bourrel et al., 2015). Examining higher elevation stations increases the likelihood of seeing snow as the dominant precipitation type instead of intense seasonal rainfall. Moreover, remote high-elevation watersheds are more likely to be free of any

geomorphological alterations, such as damming or other construction that can impact how snow is built up and how water flows out of watersheds (Ye et al., 2003). In practice, this elevation threshold aimed to limit the number of abnormal/difficult to work with hydrographs (see Section 6.2 for more information). Following these steps, 207 SNOTEL stations remained, and these make up the data for the first hypothesis of this study (**Figure 2)**.

Secondly, an elevation threshold of 2500 meters was also implemented. This second filtering process was chosen as a means of examining how the April 1 assumption varied as a function of elevation. After this second filter, only 121 SNOTEL stations remained (see **Figure 3**), and these were the final SNOTEL stations used in the remaining analyses.

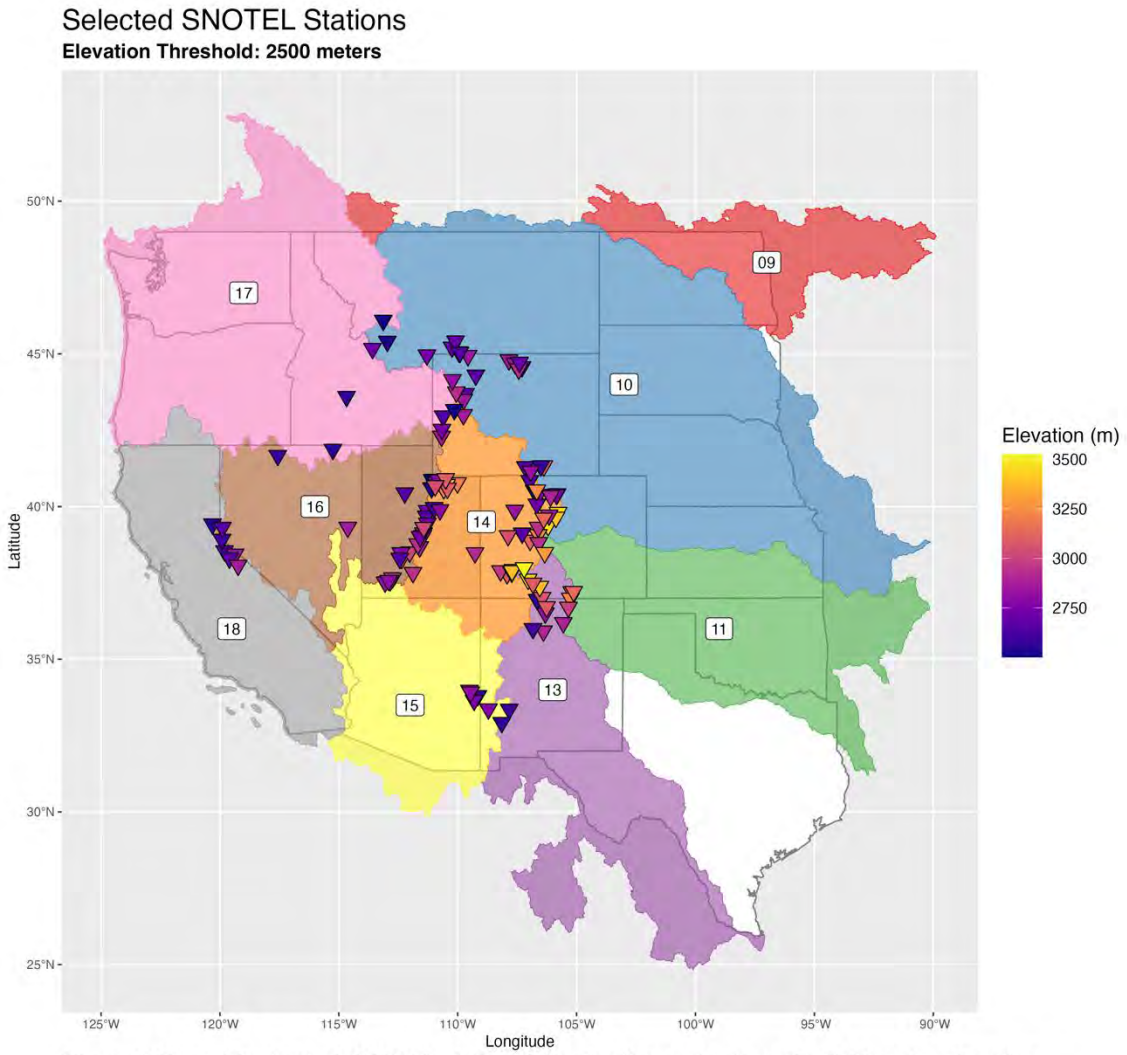

Figure 3 Map of final set of SNOTEL stations following the application of a 2500-meter elevation filter. Total number of stations is 121, colored by elevation. Shaded regions are large river basins (HUC2s) that are numbered here.

3.2 Daily Mean Streamflow Data

Daily mean streamflow data were collected in the same spatial distribution as those of SWE and air temperature. These variables, collected from the SNOTEL network as described in Section 3.1, are measured at 897 sites (the total number in the whole network), each of which is part of a small watershed, or in USGS terminology, HUC8. HUC8 stands for 'Hydrologic Unit Code', with

‘8’ denoting the size of the watershed. The larger the number, the smaller the watershed. The SNOTEL data all together (pre-filtering) encompass approximately 270 HUC8s.

Daily mean streamflow data were collected from the United States Geological Survey’s Water Data Dashboard (https://waterdata.usgs.gov/nwis?) by employing the ‘dataRetrieval’ package in RStudio (De Cicco et al., 2023). The goal behind the collection of these streamflow data was as follows: to understand how much water (as fluvial discharge) is leaving each small watershed (HUC8). Therefore, it was pertinent to measure the daily mean streamflow at the outflow point of that watershed. Moreover, each HUC8 may contain several SNOTEL stations, each of which will release its water as snowmelt during the start of the spring thaw. It was vital then to collect a representative value for the snowmelt of that entire HUC8, because it is the sum of all of the snowmelt in that catchment. To address this, the ‘dataRetrieval’ R package was utilized to select the USGS stream gauge that drained the largest area of that HUC8, the outflow point. Consequently, the daily mean streamflow values are representative of the cumulative streamflow that is leaving that catchment through the stream channel.

The data filtering process described in Section 3.1 at first left 99 USGS streamflow gauges (99 HUC8s) with the 2000-meter elevation minimum, and then only 69 USGS stream gauges with the 2500-meter minimum, a considerably smaller count compared to the number of SNOTEL stations (**Figure 4**). This is due to the fact that several SNOTEL stations can be contained in one

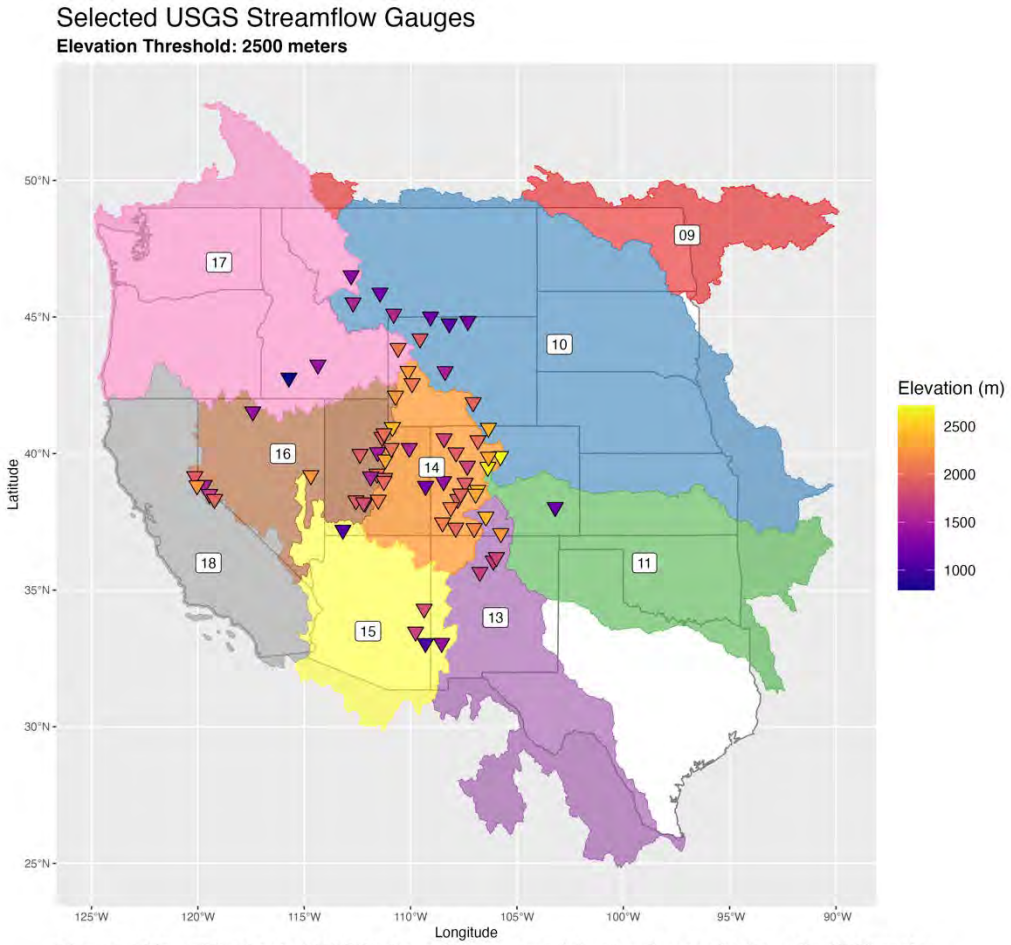

Figure 4 Map of final set of USGS streamflow gauges following the application of a 2500-meter elevation filter. Some gauges are below 2500 meters because the threshold was applied to the SNOTEL stations whose melt can be drained below 2500 meters. Total number of gauges is 69, colored by elevation. Shaded regions are large river basins (HUC2s) that are numbered here.

single small watershed, and thus have the same assigned streamflow time series. Note that despite an elevation filter of 2500 meters being applied, it does not remove all USGS streamflow monitoring stations below an elevation of 2500 meters. The same can be said for the elevation minimum of 2000 meters. The filter was applied to all SNOTEL stations, and the USGS streamflow monitors selected are placed at the outflow points of each small watershed (HUC8), each of which can span hundreds to thousands of meters of elevation. Snow that falls at an elevation of 3000 meters can leave the watershed as snowmelt hundreds of meters below where it fell, resulting in the discrepancy described between **Figures 3** and **4**.

3.3 Snowpack, Streamflow, and Other Characteristics

There were a number of different characteristic time series that were collected or computed from the data. Each of these characteristic time series were computed at all SNOTEL stations (with joint characteristics computed for the corresponding USGS streamflow gauges that drain the measured SWE). Note that for date characteristics, values were converted into a numeric value, the number of days since the start of the water year: October 1. This convention is easier for later computations in R than using a string or date format object (e.g., "2007-04-06" becomes 187 days from October 1).

The first data were the snowpack characteristics, and they could be pulled directly from a snowpack hydrograph such as shown in **Figure 5**. The two snowpack characteristics were the magnitude and the date of peak snowpack. As SWE generally increases over the course of the year, and then sharply drops off as temperatures rise above zero, it was trivial to select the date and magnitude of peak SWE. These snowpack characteristics were chosen to represent how much snow fell in each watershed location during each year in the 43-year time series, as well as at which time each year.

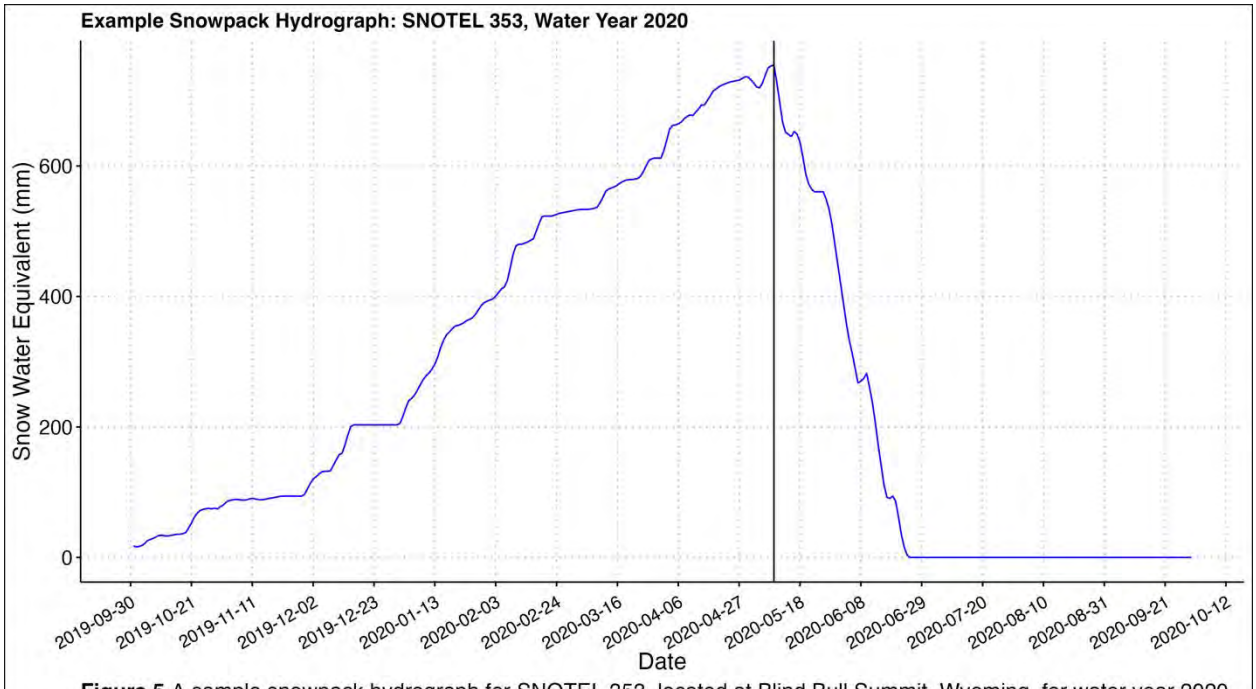

Figure 5 A sample snowpack hydrograph for SNOTEL 353, located at Blind Bull Summit, Wyoming, for water year 2020. The vertical black line represents the date of peak SWE, May 9, 2020. The magnitude of peak SWE is 754.4 mm.

Next, streamflow characteristic time series were computed and picked. A visual method was required to improve their accuracy. To understand snowmelt streamflow, as was the focus of this study, the date of snowmelt onset was selected. To do so, a four-panel plot was created for each USGS streamflow gauge (HUC8) in each year. An example of one of these panel plots is shown in **Figure 6**. In this figure, several different sets of data are plotted. From top-to-bottom, they are a smoothed SWE hydrograph (the same as in **Figure 5**) collected at one of the SNOTEL stations that resides in that HUC8, a smoothed mean daily discharge curve collected at that gauge, a cumulative frequency distribution of that year's streamflow, and the air temperature curve also collected at one of the SNOTEL stations in that HUC8. From this plot, the date of snowmelt onset was selected: the date on which the mean daily discharge significantly increased in a manner corresponding to a similar drop in SWE and the temperature rising above 0°C. In the example

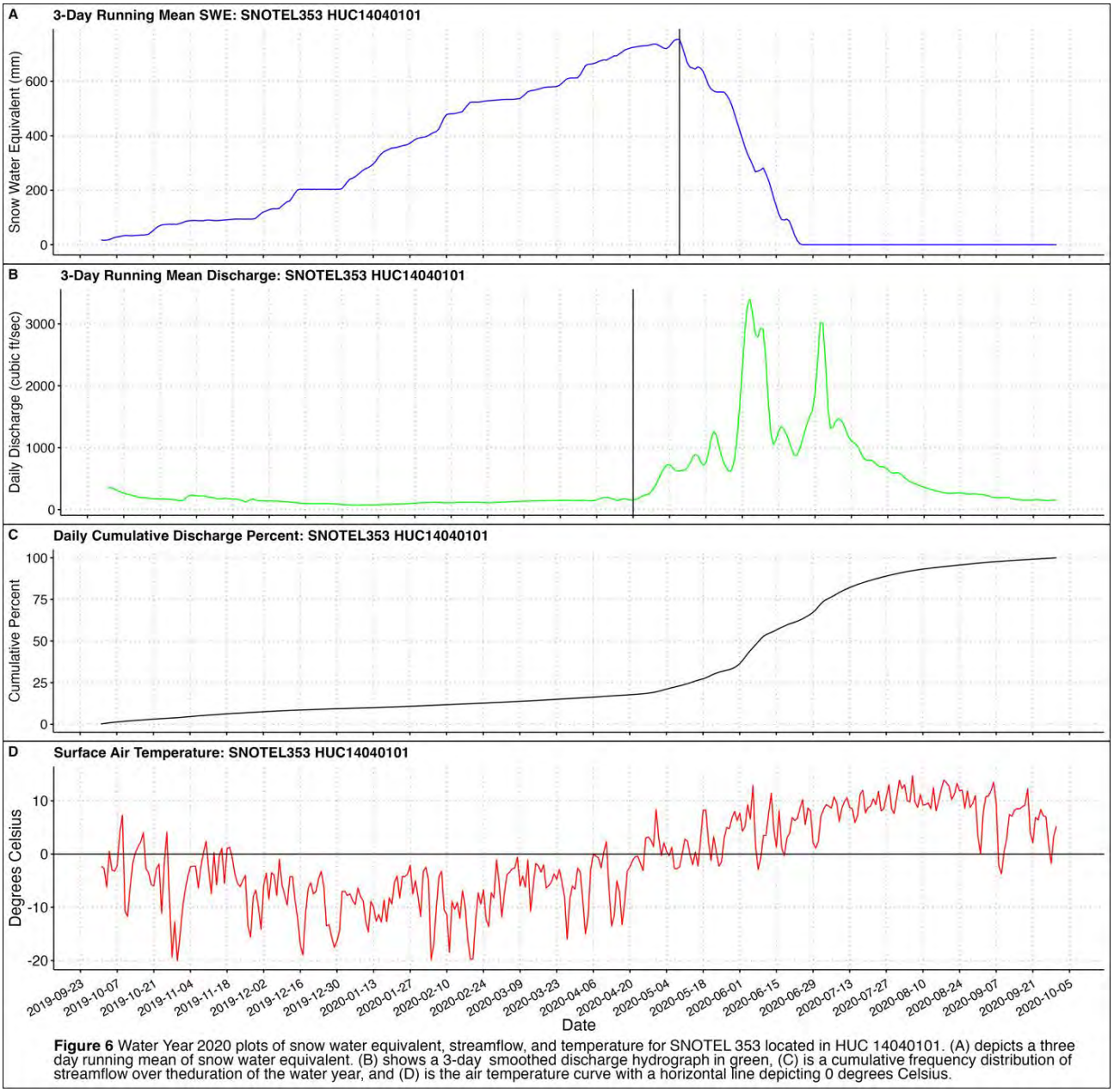

Figure 6 Water Year 2020 plots of snow water equivalent, streamflow, and temperature for SNOTEL 353 located in HUC 14040101. (A) depicts a three day running mean of snow water equivalent. (B) shows a 3-day smoothed discharge hydrograph in green, (C) is a cumulative frequency distribution of streamflow over theduration of the water year, and (D) is the air temperature curve with a horizontal line depicting 0 degrees Celsius.

shown in **Figure 6**, the date of snowmelt onset is shown by the vertical black line on the second panel, April 20, 2020.

Once selected, the snowmelt onset dates provided some information about when snowmelt flow begins, and thus narrowed the time window that the rest of the streamflow characteristics were computed from. These other characteristics were the date and magnitude of peak streamflow and the rise time. The magnitude of peak mean daily discharge was calculated and then normalized to the size of the HUC8 basin area in question. This normalization allowed for like-to-like comparisons of streamflow magnitudes. It is important to note that characteristics beyond the date of snowmelt onset were only selected if the date of snowmelt onset was selected also. Occasionally, complexities in the streamflow data prevented a confident snowmelt onset date, and these years were assigned NA values. Any characteristics that required the date of snowmelt onset were also assigned NA if no snowmelt onset date was selected. Overall, 319 of the 2760 (11.55%) individual snowmelt onset picks were undeterminable and assigned NA. These complications in snowmelt onset date selection are discussed further in Section 6.2.

Shown in **Figure 7** is an example of a streamflow hydrograph from the second panel in **Figure 6**. This hydrograph is for the USGS gauge located at the pour-point of HUC 14040101, which contains SNOTEL stations 353, 597, and 779. The vertical black line represents the date of snowmelt onset that was picked visually using the panel plot method described above: April 20, 2020. The date of peak streamflow was then the maximum value of mean daily discharge shortly after this snowmelt onset date. In this case, it was June 4, 2020, and is shown by the red line. From these two dates, the rise time can be computed, or the number of days that elapse from the date of snowmelt onset until the date of peak mean daily discharge for that year's snowmelt event. For this example, the rise time was 45 days.

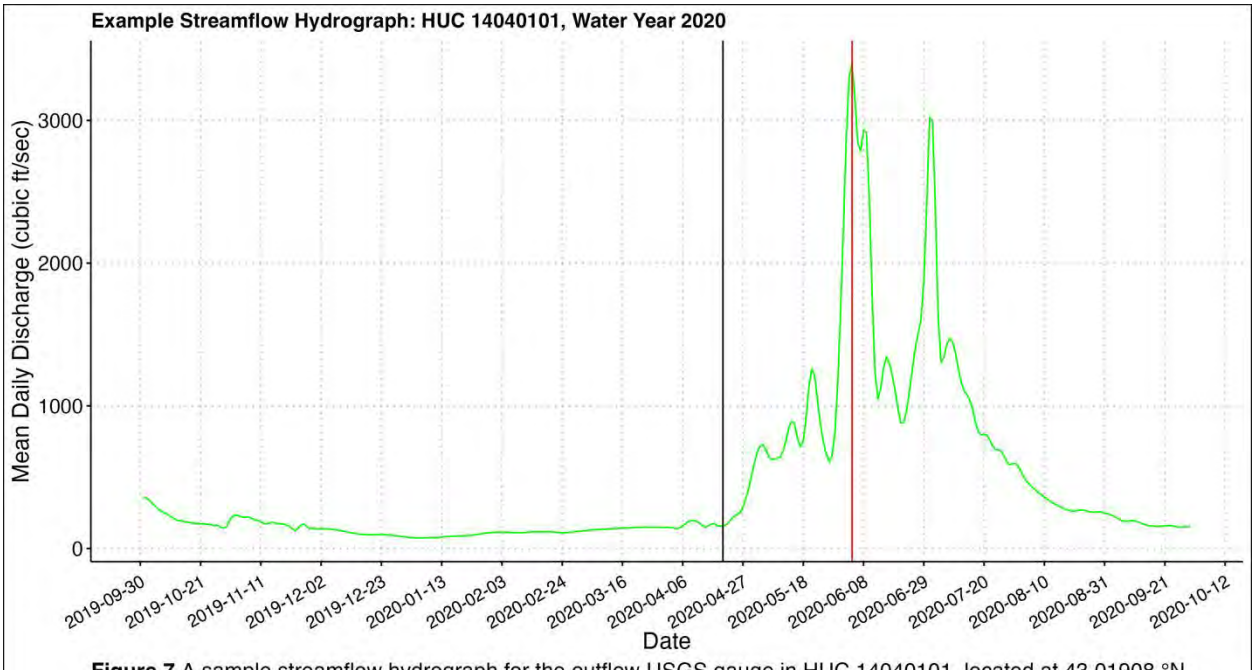

Figure 7 A sample streamflow hydrograph for the outflow USGS gauge in HUC 14040101, located at 43.01908 °N, -110.1189 °W, for water year 2020. The vertical black line represents the date of snowmelt onset, April 20, 2020. The vertical red line represents the date of peak mean daily discharge, June 4 2020.

3.4 Normalization and Binning of Streamflow

For the second part of this study, 69 individual small watersheds were considered, each of which has a different size, elevation, and location. In order to compare the results of the hydrological analyses, it was important to normalize the streamflow data and characteristics to the size of the basin. To do this, the basins were grouped into separate bins of varying watershed size. HUC8 basin areas were collected along with the streamflow data themselves, and converted from units of cubic miles to cubic kilometers. Likewise, mean daily discharges were converted to cubic meters per second from cubic feet per second. There was a wide range of HUC8 drainage areas, from less than 500 square kilometers, up to nearly 70,000 square kilometers. Consequently, each basin drained a different amount of water depending on its size, its snowfall, and its location as well. Six individual bins were created.

3.5 Statistical Methods

In order to explore the April 1 assumption, several simple statistics were computed on the date of peak snowpack data. These data were computed for each water year at all of the SNOTEL stations in each phase of the work. Recall that first, a 2000-meter elevation threshold was applied, leaving 207 SNOTEL stations. Next, a 2500-meter minimum was put in place, leaving only 121 individual SNOTEL stations.

Dates of peak snowpack were subtracted from April 1, giving a number of days difference from April 1. The means, standard deviation, skewness, and kurtosis were computed in R for each decade in question in the time series (1980s, 1990s, 2000s, and 2010s including 2020-2022). These statistical measures are various descriptors of the shape and character of a distribution. Next, a non-parametric t-test called the Wilcoxon Test was applied to determine if the overall sample mean was statistically significantly later from April 1. The Wilcoxon Test is part of the 'stats' package in R and was specified to be a one-sample test compared to the mean to be tested: April 1 or 0 days difference (R Core Team, 2023). The test was performed at the 95% confidence level.

Following the Wilcoxon Test, the Mann-Kendall test for trend was performed on each of the characteristic snowpack time series, first with the sample of 207 SNOTEL stations, and then with the further filtered 121 SNOTEL stations. The Mann-Kendall tests were performed in R using the 'Kendall' package, and it was assumed that the computed characteristic time series were independent from one year to the next (McLeod, 2011). The Mann-Kendall test is useful for determining a monotonic (not-necessarily linear) trend in a set of data. In this case, the p-value produced was considered significant when $p < 0.05$. For significant trends, the direction was determined by the 'tau' value provided with the test result. For $tau > 0$, the trend was increasing, and for $tau < 0$, the trend was decreasing.

4.0 Results

4.1 Testing the April 1 Assumption

In order to first test the April 1 assumption for the date of peak snowpack, the dates of peak SWE were computed for all 43 water years at all 207 SNOTEL stations. Again, these 207 SNOTEL stations were those that remained following the application of a 2000-meter elevation filter. These are shown in **Figure 8**, broken down by each decade. Note that the full sample mean is approximately 5 days after April 1, and the peak SWE dates are not uniformly distributed, nor are they overly-similar across decades. A one-sided Wilcoxon test for non-parametric means was performed on the dates of peak SWE (with respect to April 1, where 0 represents April 1). At the

95% confidence level, the null hypothesis, that the mean is not significantly later than April 1, was rejected ($p < 0.001$).

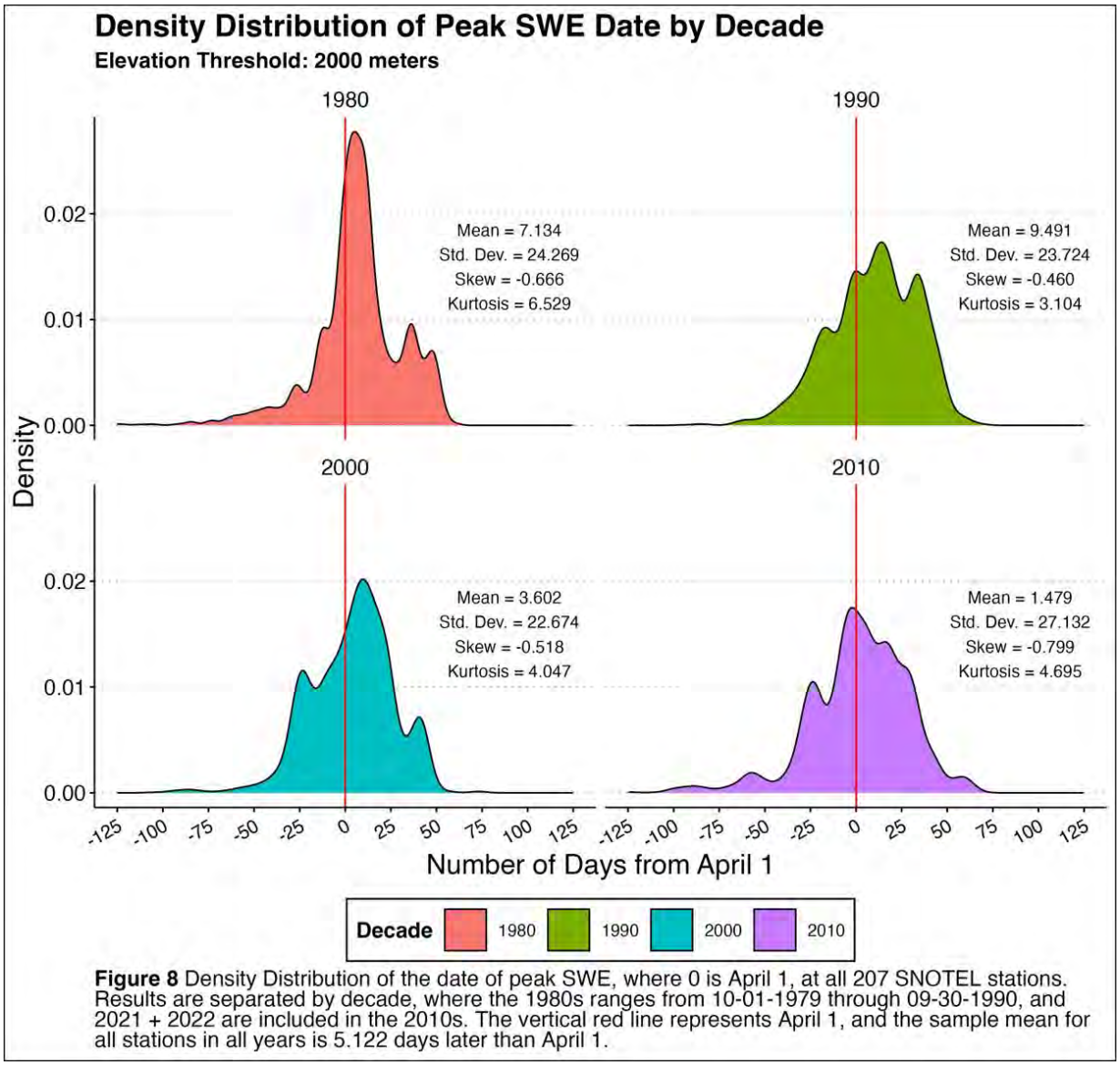

Figure 8 Density Distribution of the date of peak SWE, where 0 is April 1, at all 207 SNOTEL stations. Results are separated by decade, where the 1980s ranges from 10-01-1979 through 09-30-1990, and 2021 + 2022 are included in the 2010s. The vertical red line represents April 1, and the sample mean for all stations in all years is 5.122 days later than April 1.

Shown in **Figures 9** and **10** are Mann-Kendall maps of the 207 SNOTEL stations, first for the magnitude of peak SWE, and second for the April 1 SWE value. The Mann-Kendall test was performed on each of the characteristic time series that was produced at each station, and trend was determined to be significant for $p < 0.05$. Increasing trends are indicated by blue dots, decreasing trends by red dots, and no trend is indicated by grey dots. In **Figure 9**, most of the SNOTEL stations displayed insignificant trends in their peak snowpack, and 49 stations displayed decreasing trends in the magnitude of peak SWE over the 43-year time period. **Figure 10** shows the Mann-Kendall trend test results for the value of April 1 SWE. Again, the majority of the stations showed insignificant SWE magnitude trends, with only 47 stations displaying a negative trend in April 1 SWE. Respectively, these represent 23.6% and 22.7% of the sample that experienced significant decreases in snowpack over the time period 1980 through 2022. One key difference between the two sets of Mann-Kendall tests (for Peak SWE and April 1 SWE) was the slight northerly-bias that was produced in the April 1 SWE dataset. Approximately 5 high-latitude stations that were insignificant in the peak SWE result became significant using the April 1 assumption.

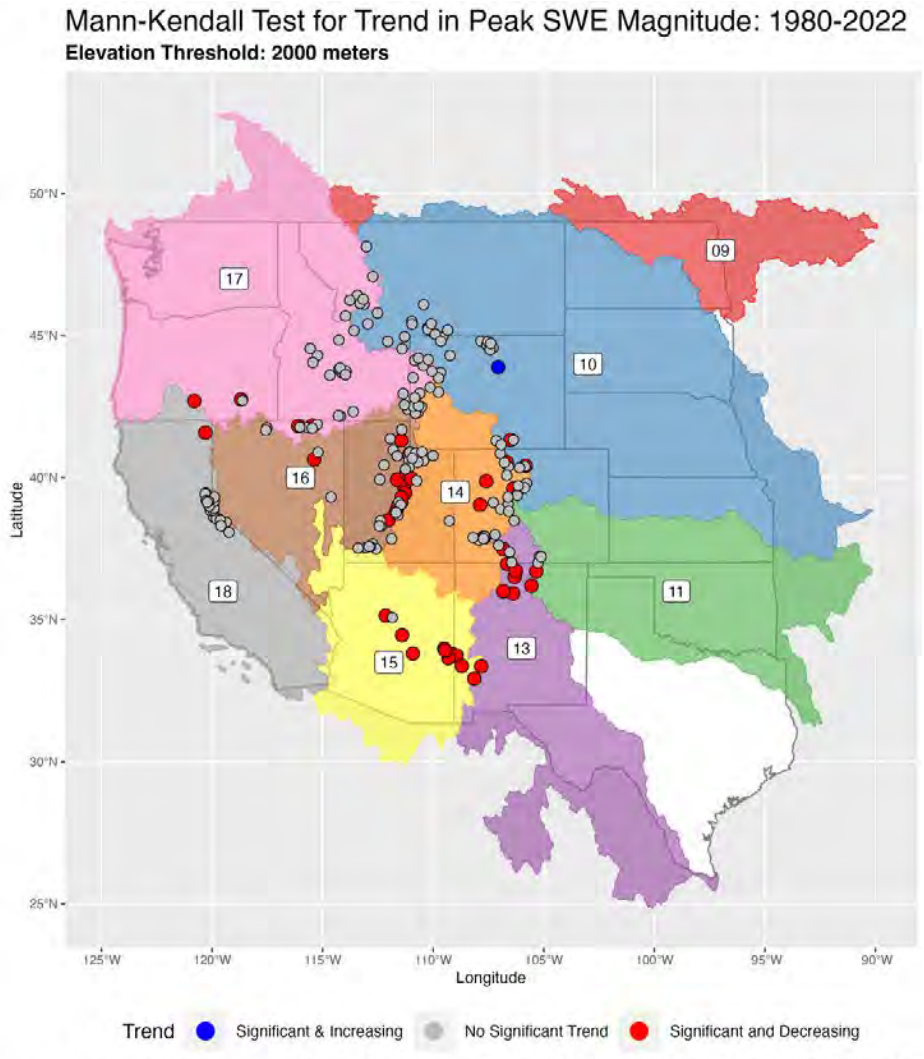

Figure 9 Non-Parametric Mann-Kendall Test for Trend of the Peak SWE Magnitudes at all 207 SNOTEL stations. Mann-Kendall Test performed at the 95% Confidence Interval. Significance determined when $p<0.05$. Blue dots represent stations that have a significant increasing trend, red dots significant and decreasing. Grey dots represent stations with no significant trend.

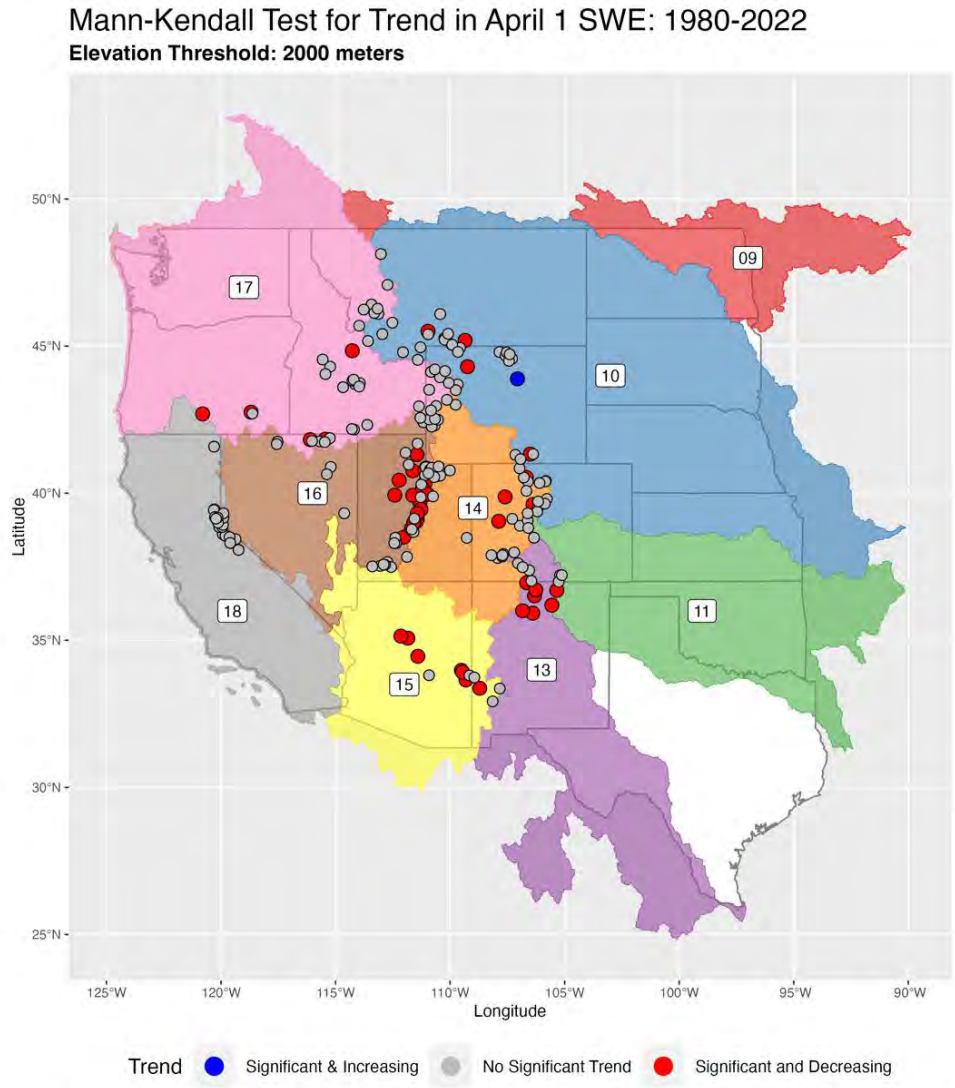

Figure 10 Non-Parametric Mann-Kendall Test for Trend of the Peak SWE Magnitudes at all 207 SNOTEL stations. Mann-Kendall Test performed at the 95% Confidence Interval. Significance determined when $p<0.05$. Blue dots represent stations that have a significant increasing trend, red dots significant and decreasing. Grey dots represent stations with no significant trend.

Next, the 2500-meter elevation threshold was implemented, and the same tests were performed on this new set of 121 SNOTEL stations. The date of peak SWE distributions are shown in **Figure 11**. The Wilcoxon test suggested that the mean date of peak SWE for the 43 years is significantly later than April 1 ($p < 0.001$) and significantly later than April 9 ($p = 0.0012$). The overall sample mean date of peak SWE was April 10. **Figure 12** and **13** show the updated Mann-Kendall results for the same 121 SNOTEL stations. In the case of the date of peak SWE, 32 SNOTEL stations displayed significant decreasing trends. For April 1 SWE, the number of significant decreasing trends was 27 SNOTEL stations. Respectively, these represent 26.4% and 22.3% of the sample that experienced decreases in their snowpack from 1980 through 2022.

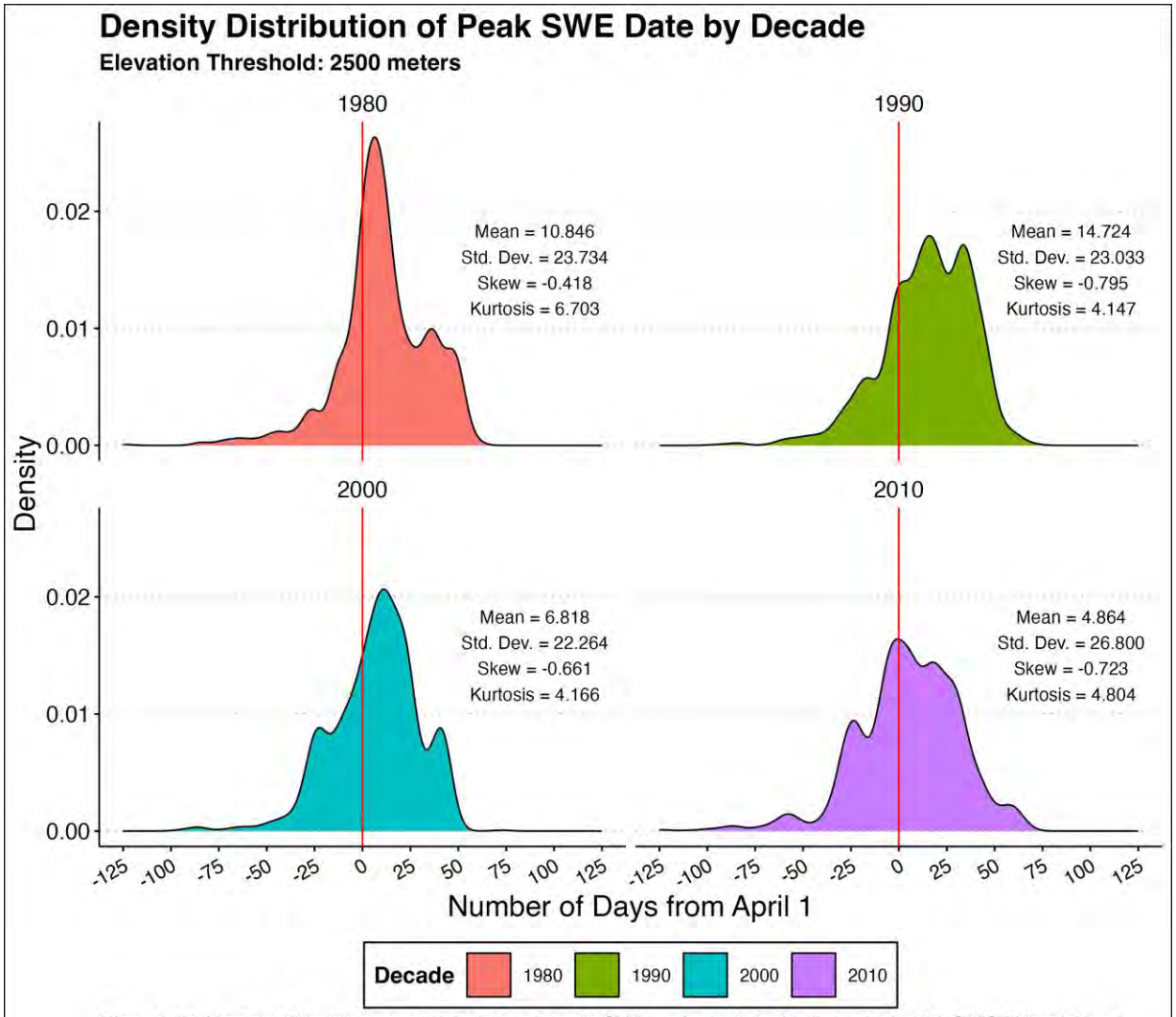

Figure 11 Density Distribution of the date of peak SWE, where 0 is April 1, at all 121 SNOTEL stations. Results are separated by decade, where the 1980s ranges from 10-01-1979 through 09-30-1990, and 2021 + 2022 are included in the 2010s. The vertical red line represents April 1, and the sample mean for all stations in all years is 8.978 days later than April 1.

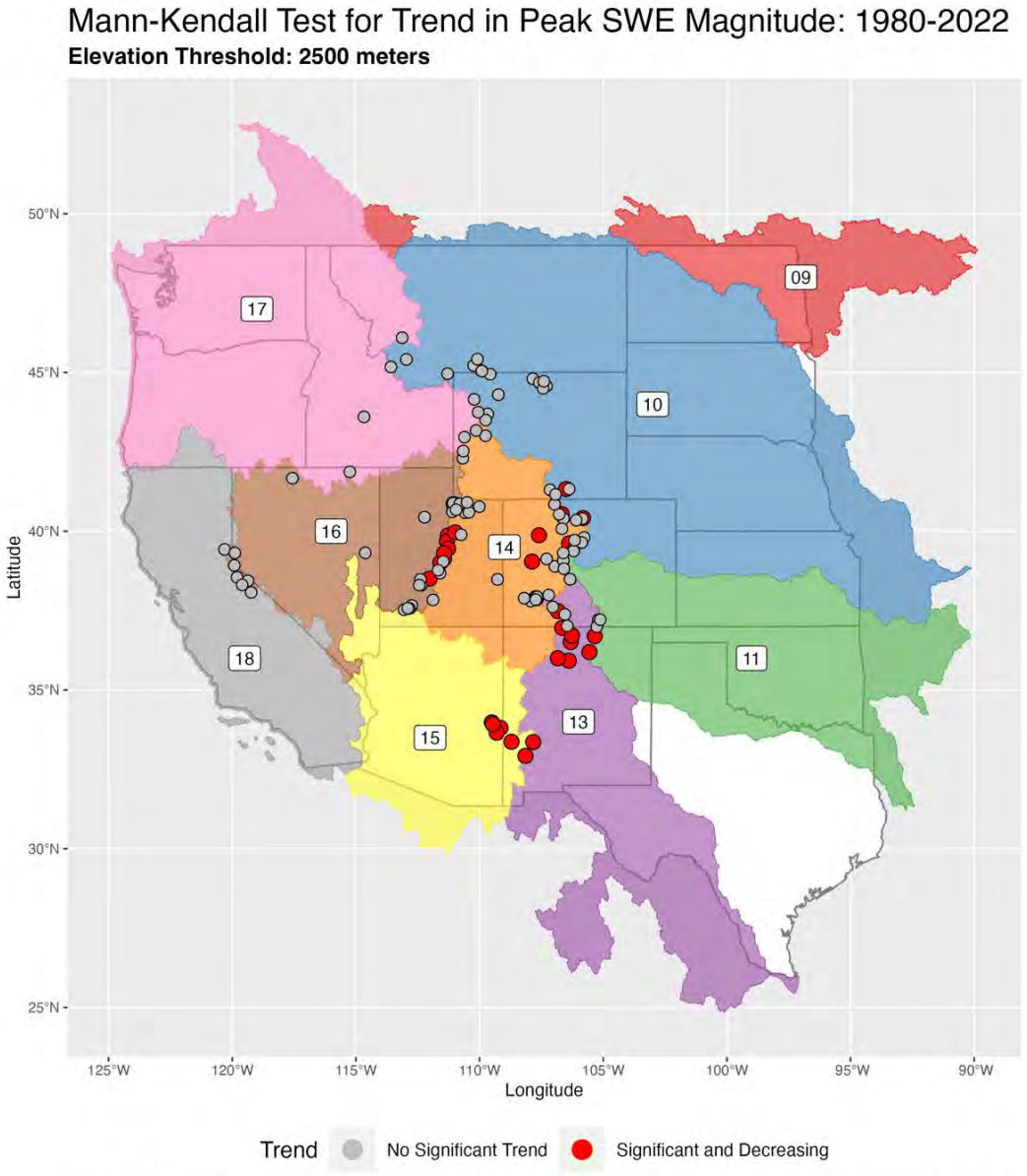

Figure 12 Non-Parametric Mann-Kendall Test for Trend of the Peak SWE Magnitudes at all 121 SNOTEL stations. Mann-Kendall Test performed at the 95% Confidence Level. Significance determined when $p<0.05$. Blue dots represent stations that have a significant increasing trend, red dots significant and decreasing. Grey dots represent stations with no significant trend.

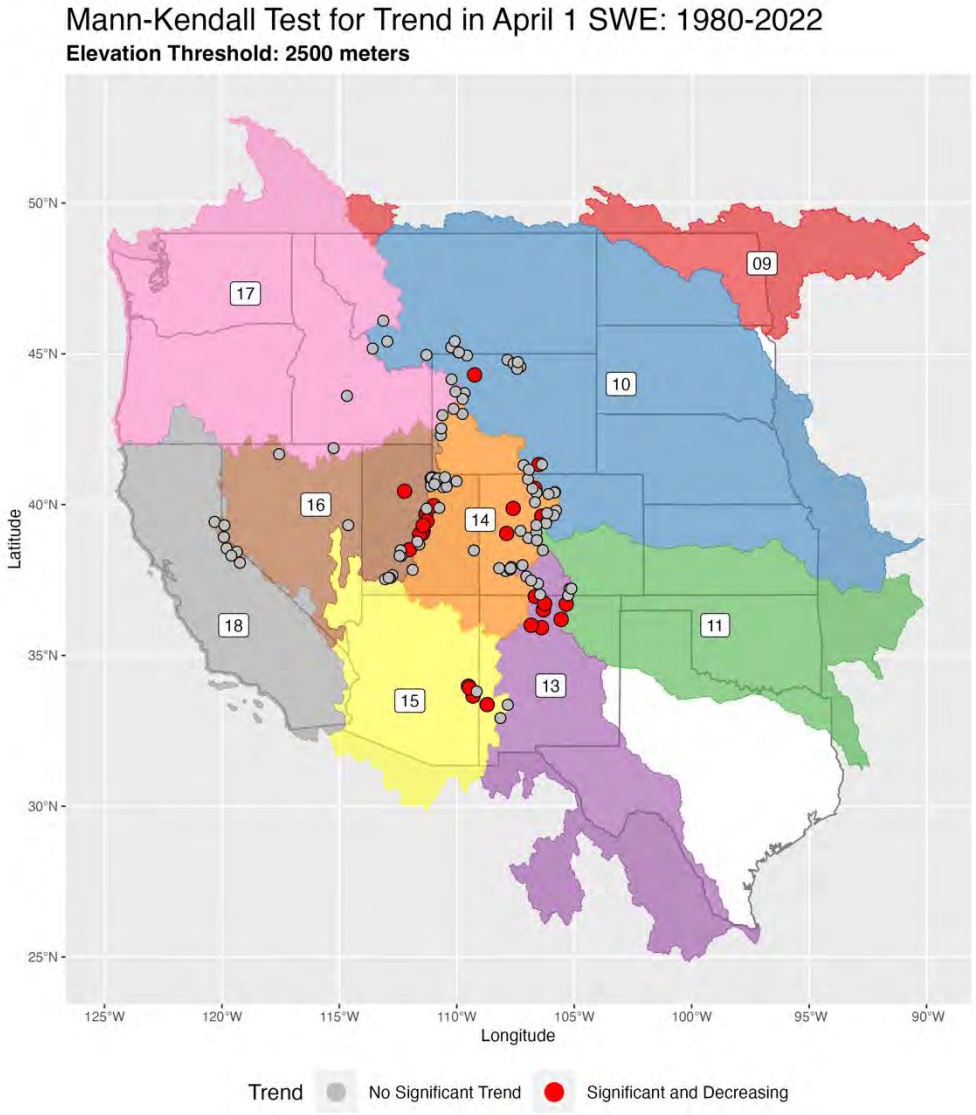

Figure 13 Non-Parametric Mann-Kendall Test for Trend of the Peak SWE Magnitudes at all 121 SNOTEL stations. Mann-Kendall Test performed at the 95% Confidence Level. Significance determined when $p<0.05$. Blue dots represent stations that have a significant increasing trend, red dots significant and decreasing. Grey dots represent stations with no significant trend.

4.2 Hydrograph Variability

Following the results of the Wilcoxon and Mann-Kendall tests, the 2500-meter threshold was kept in place, and a number of relationships were explored between the different variables that had been computed and collected. With the 2000-meter threshold, trends were unclear between different variables.

Shown in **Figure 14** is the magnitude of peak SWE plotted against the date of peak SWE for each year. The plot was divided into 6 different drainage area bins. The points are colored by their latitude, and each of the bins display a similar pattern. Higher latitudes (i.e., northern

SNOTEL stations) had later peak SWE dates that were generally no later than the first week of June. The 1000-5000 km^2 bin had the most variability in the magnitude of peak SWE, reaching as high as nearly 2.5 meters. Each bin displayed a similar shape, reminiscent of an exponential growth curve, particularly in the middle-sized basins. In the smallest watersheds, latitudinal trends were unclear, and the same can be said for the 10000-20000 km^2 bin.

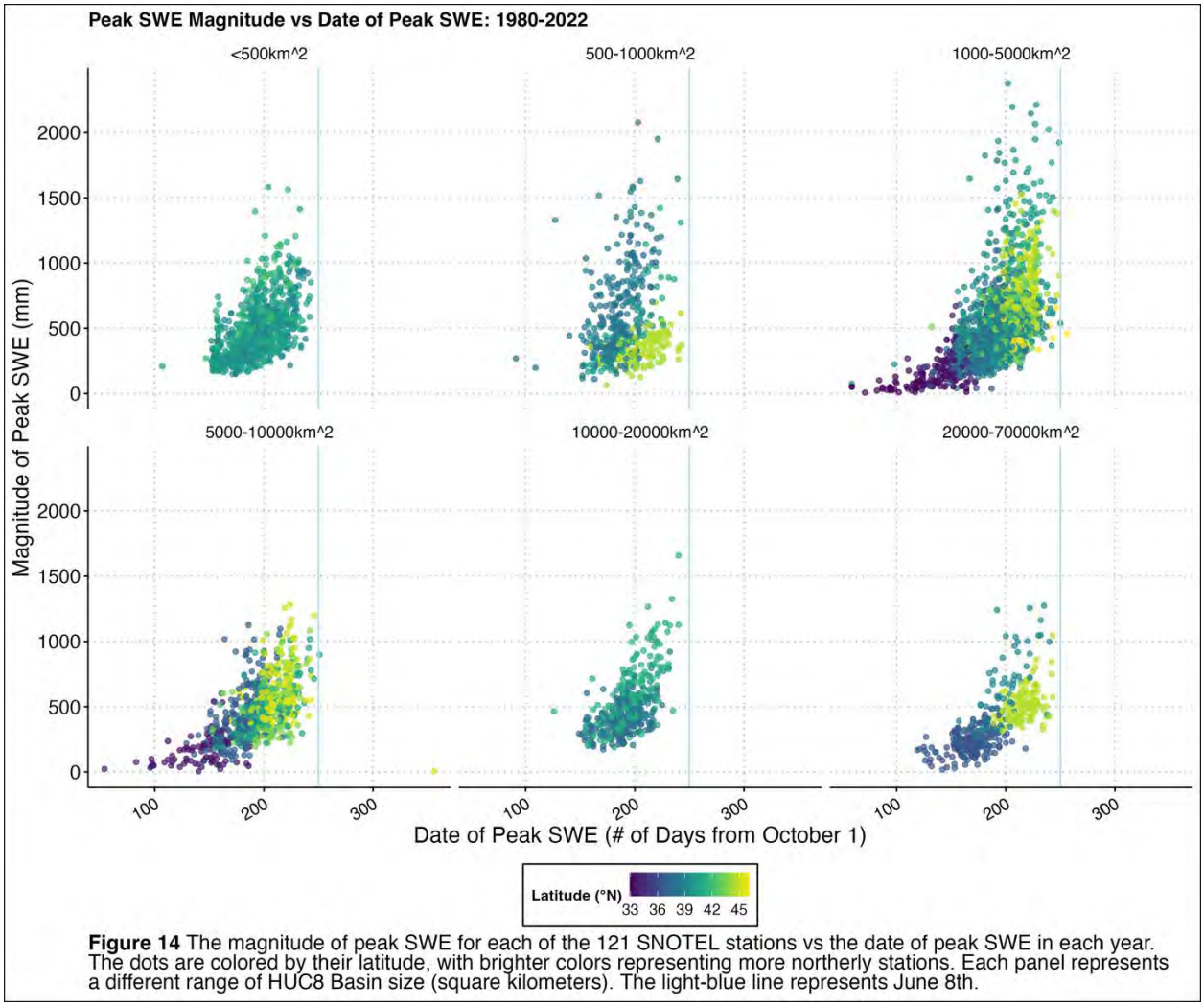

Figure 14 The magnitude of peak SWE for each of the 121 SNOTEL stations vs the date of peak SWE in each year. The dots are colored by their latitude, with brighter colors representing more northerly stations. Each panel represents a different range of HUC8 Basin size (square kilometers). The light-blue line represents June 8th.

Figure 15 displays the distributions of the dates of snowmelt onset that were picked following the methodology outlined in Section 3.3. Each boxplot represents a different drainage area watershed, from small to large. All of the boxplots tended to have more outliers on the early side, but the median is generally around the beginning of April. The mean snowmelt onset for the whole sample was April 9, similar to the average date of peak snowpack. The standard deviation was 25 days, the skewness -0.214, and the kurtosis 3.429. More summary statistics are summarized in **Table 1.** From this table, there are no clear trends in snowmelt onset with basin area.

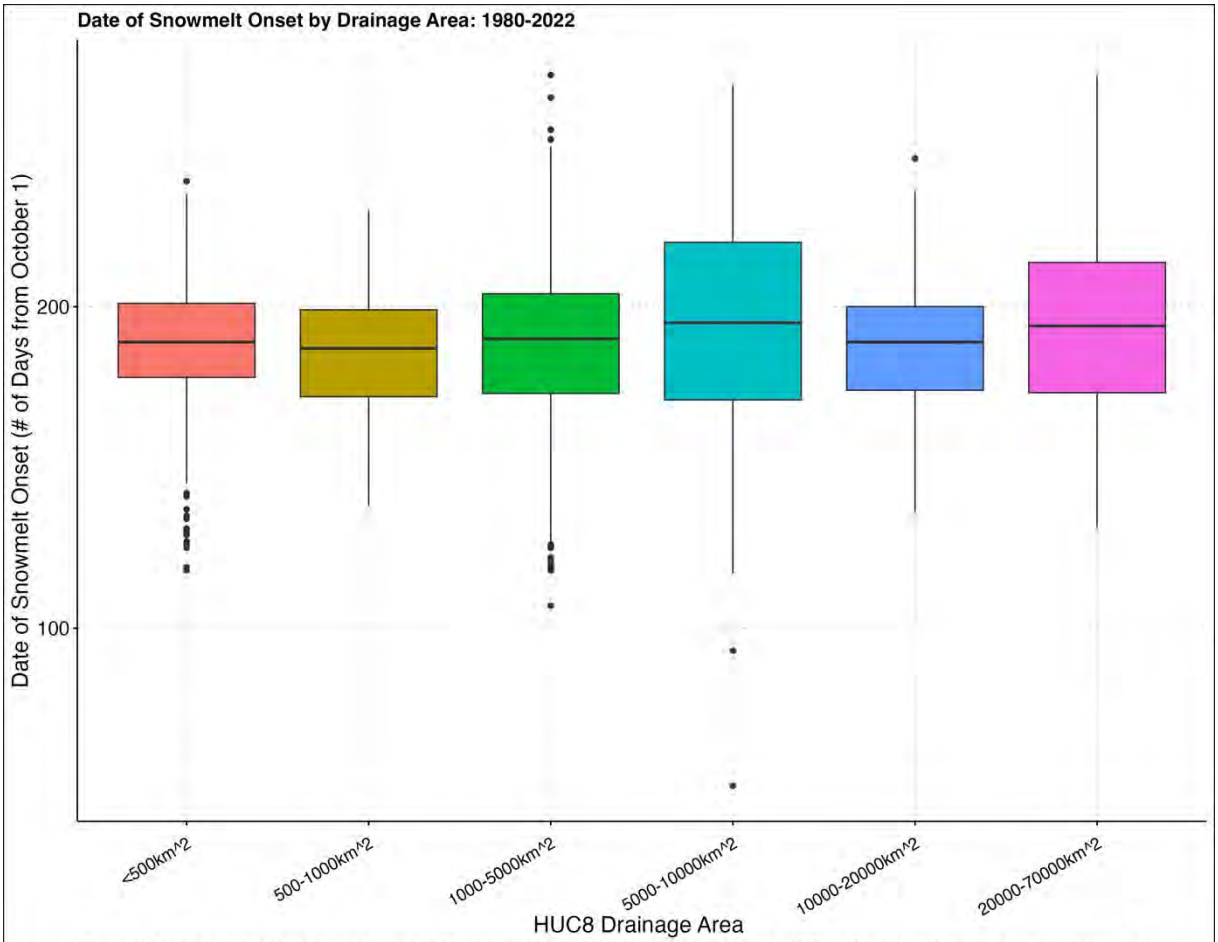

Figure 15 The date of snowmelt onset for each of the 121 SNOTEL stations (69 watersheds) vs the basin drainage area. On the y-axis, 200 days from October 1 corresponds to April 19. From left to right, the number of SNOTEL stations in each bin is: 24, 11, 47, 19, 10, 9.

Drainage Area	# of HUC8s	Mean	Median	Standard Deviation	Interquartile Range
< 500 km^2	14	April 9	April 8	20 days	23 days
500-1000 km^2	8	April 6	April 6	19 days	27 days
1000-5000 km^2	29	April 8	April 9	26 days	31 days
5000-10000 km^2	8	April 13	April 14	33 days	49 days
10000-20000 km^2	5	April 3	April 8	20 days	26 days
20000-70000 km^2	4	April 12	April 13	27 days	41 days

Table 1 Summary statistics for snowmelt onset dates. Dates were picked with respect to October 1. NA values were removed when computing the statistics. Statistics were rounded to the nearest day.

Figure 16 displays peak mean daily discharge versus the magnitude of peak SWE, also broken down by drainage basin size. Again, there was a notable relationship with station latitude. Lower latitude stations tended to have more chaotic (less defined) relationships with the magnitude of peak SWE. Higher latitude stations, however, showed more clearly defined slopes, most notably for basins with area 1000-5000 km^2 and 5000-10000 km^2. For these basin sizes, maximum streamflow increased linearly with the magnitude of peak SWE. For the smallest basins, southern and northern stations tended to have similar and less predictable relationships with snowpack magnitude.

No relationship was observed between rise time (the duration from snowmelt onset to peak snowmelt discharge) and drainage basin size, although it was hypothesized that there would be a directly proportional relationship. Even with this high-elevation threshold, trends and relationships did not appear readily apparent, particularly some of the later streamflow characteristics, including the date of peak mean daily discharge. There was a clear relationship between peak discharge and basin area. **Figure 17** displays boxplots of peak discharge (cubic meters per second) versus the basin area (square kilometers). Note the logarithmic scale on the y-axis. This relationship is expected, as a larger basin will drain more water and thus have larger discharges at its pour point.

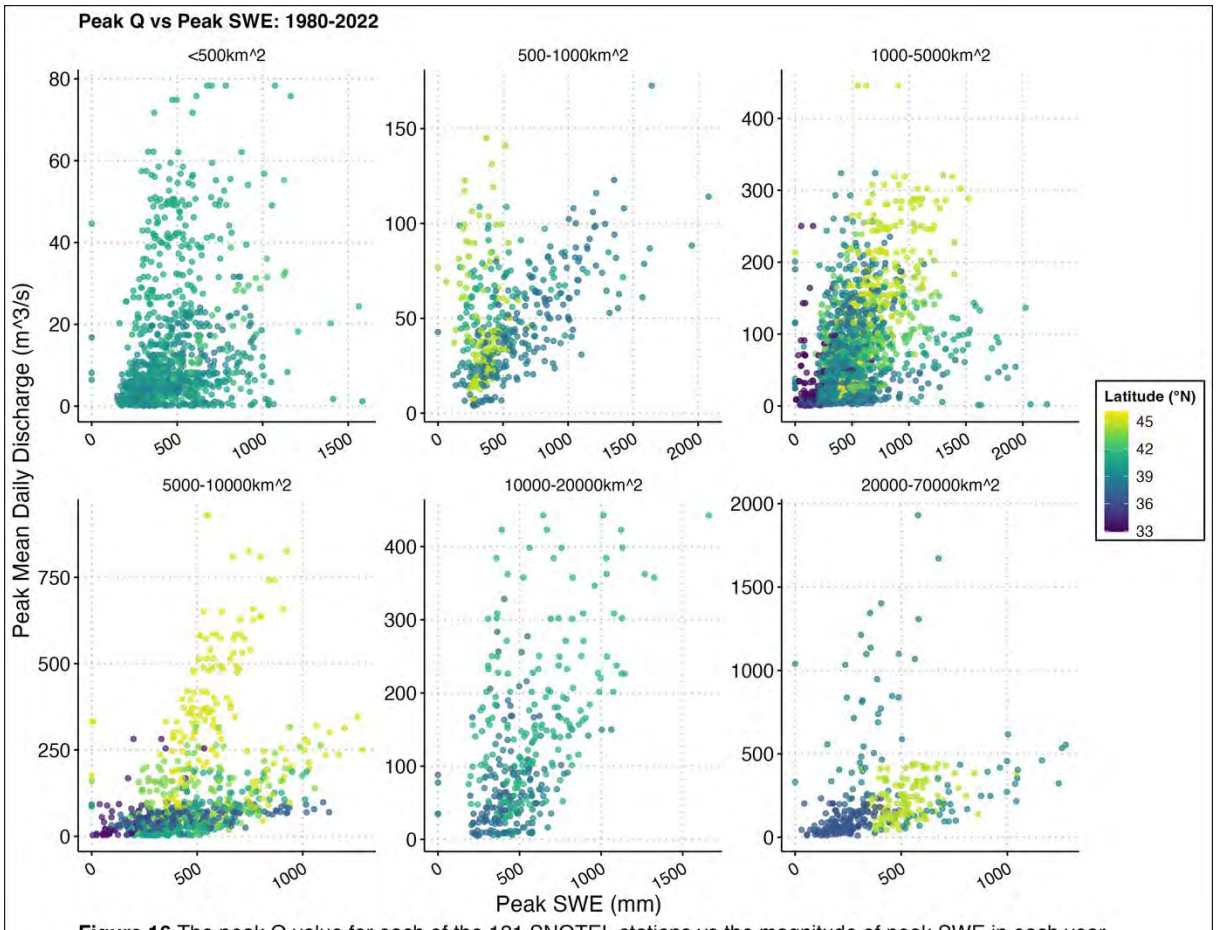

Figure 16 The peak Q value for each of the 121 SNOTEL stations vs the magnitude of peak SWE in each year. The dots are colored by their latitude, with brighter colors representing more northerly stations. Each panel represents a particular drainage area, with the y-axis corresponding to the peak Q value measured in cubic meters per second.

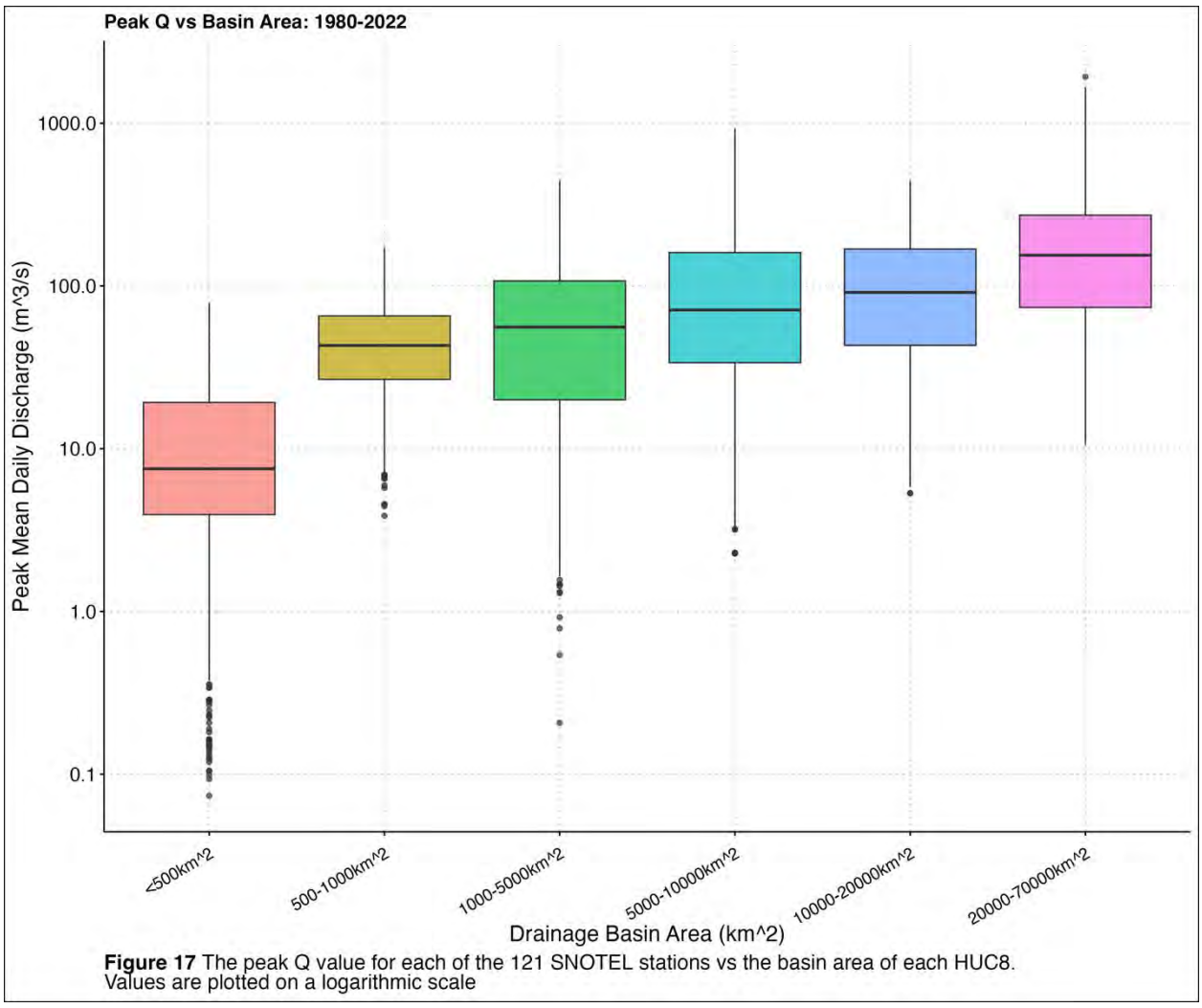

Figure 17 The peak Q value for each of the 121 SNOTEL stations vs the basin area of each HUC8. Values are plotted on a logarithmic scale

5.0 Discussion

This work set out to examine four main hypotheses. *Hypothesis 1* was that the selection of April 1 as the date of peak SWE imparts systematic underestimations of the magnitude of peak SWE, particularly at high elevation sites. In this paper, it was found that for high elevation sites, the April 1 assumption *was* statistically later than April 1 from 1980 through 2022. However, at elevation thresholds of 2000 meters and 2500 meters, the earlier years in the record deviated further from April 1 and approached April 1 into the 2000s. From these results, it is apparent that the April 1 assumption does not tell the whole story. With the 2500-meter threshold, the April 1 assumption was even more inaccurate than the lower elevation sample. This indicates, as hypothesized, that choosing to not use the true date of peak snowpack when computing snowpack patterns underestimate the true magnitude of peak SWE.

In keeping with this line of thought, *Hypothesis 2*, that the April 1 assumption can mask true snowpack trends and patterns, was also investigated. **Figure 1,** from the U.S. EPA, was constructed using the April 1 methodology outlined in several papers (Mote et al., 2004; Mote, 2006; Mote et al., 2018). This study featured similar maps (**Figures 9, 10, 12, & 13**). In examining these figures, it is clear that they are not particularly similar. While this study saw many significant

decreasing trends in both the April 1 and true peak SWE date via Mann-Kendall computations, the majority of the stations did not display a significant trend in either direction. This is the most notable difference between the results of this paper and the results of **Figure 1**. For one, this study considered far fewer locations: the U.S. EPA data did not include an elevation filter. As mentioned earlier, snow/rain ratios have been most susceptible to change in the lower elevations, where temperatures are higher (Knowles et al., 2006). This, along with other human influences that are more likely at lower elevations, is probably the most direct driver of the trends displayed in **Figure 1**. Along with the lack of elevation filter, the results of **Figure 1** represent snowpack trends over a considerably longer time period: 1955-2022. This study focused on 1980-2022, and consequently is likely to see fewer decreasing trends. If it is assumed that snowpacks have been decreasing under the warming climate regime throughout since at least the 20th century, it only makes sense for a longer-term study to reveal more significant decreasing snowpack trends.

With that said, if we consider just the high-elevation sites, the trends in the EPA figure and those produced in this work are still dissimilar. I discussed the snow/rain ratio decrease that is occurring at lower elevations previously. This trend has likely not yet had much of an effect at the highest elevations, where temperatures still remain below freezing for much of the year. This is supported by Knowles et al. (2006), who found that the locations in their study above 2000 meters were more resistant to decreases in the snow/rain ratio. While this study found a considerable number of high-elevation locations that did not have significant decreasing trends in both the April 1 SWE and the peak SWE, the April 1 assumption *did* have a statistically significant impact on the trends that were observed. There was also a marginal northward shift in decreasing trends when the April 1 assumption was applied, although this was not explored statistically in this work.

Several hypotheses on the relationships between the various snowpack and snowmelt characteristics were explored. It was hypothesized that peak snowmelt discharge would increase with basin area at the high latitudes and elevations (*Hypothesis 3*). This study found, as expected, that the peak streamflow increased rapidly with basin size, although the elevation/latitude differences were not as clear. The likely reason for this is the broad variability in basin areas and the fact that the basins in question could span large elevation ranges.

Furthermore, it was hypothesized that the rise time (the duration from the identified snowmelt onset to the date of peak discharge) would increase with basin area (*Hypothesis 4*). This relationship was not observed in any of the subsets of data. Basin drainage density and size were thought to contribute to the time it takes for discharges to build-up and reach their peak, but in this paper, those effects were not seen. A potential reason for this is the broad heterogeneity in the basin size within bins, i.e., the drainage area bins selected were too large. Moreover, perhaps these effects were masked by the seemingly consistent snowmelt onset times that were selected.

As stated before, the purpose of the elevation threshold in this work was to eliminate the impact of human influence on watersheds, and to maximize the likelihood that the system in question was snow-dominated. However, with the 2000-meter threshold, the streamflow hydrographs were generally too complex to make snowmelt onset picks, particularly in the more arid regions of the American west. The USGS streamflow gauges in areas such as Arizona, New Mexico, and the north-western Rocky Mountains often saw streamflow hydrographs that were clearly influenced by heavy rains in the winter and very early spring. These rains, in conjunction with weaker snowpacks (particularly in Arizona and New Mexico) muddled the streamflow hydrographs and made snowmelt onset picks impossible to make with any confidence.

To address these issues, I focused the snowpack and snowmelt analyses on SNOTEL stations above an elevation threshold of 2500 meters. Not only did this threshold clarify the

influence of the April 1 assumption, but it also eliminated many of the problematic hydrographs in the regions mentioned previously. It was hypothesized (*H3*) that elevation would play a large role in the relationships between variables, but this could not be evaluated for lower elevations. Indeed, elevation influenced the ability to define the onset of the snowmelt hydrographs. For the SNOTEL stations located at or above 2500 meters, latitude and basin area were investigated to determine their impacts on snowmelt runoff responses.

Latitude had an effect on both peak snowpack and peak snowmelt discharge. Basin size was also a factor, and grouping streamflow responses by both basin area and latitude illustrated these relationships. Latitude affects both temperature and spatial distribution of common weather patterns. The southwest is generally more arid than the northwest, and as a result tends to receive less precipitation through the winter. Large synoptic weather patterns often originate in the Pacific Northwest, and strong orographic lifting through the Rocky Mountains brings large amounts of snow to the northern reaches of the study area. The northern latitudes examined in this work tended to receive later and more substantial snowpacks and thus have more snowmelt to provide water for dry summer months.

6.0 Limitations and Uncertainties

In hydrologic studies such as this one, there are multiple sources of uncertainty and error that must be addressed. This section walks through each of the affected components of this research, and provide both reasons for uncertainty and ways in which they were addressed to increase the validity of the results.

6.1 Uncertainty in the Raw Data: SWE, Discharge

This study utilized two sources of data, each of which had an uncertainty associated with its measurement. Firstly, the SNOTEL data (snow water equivalent and air temperature) had reported uncertainties in measurement of $\pm$ 0.1 inches (2.54 mm) for SWE and $\pm$ 0.1 ºC for air temperature, respectively. These recorded uncertainties are small, and in the context of this work, did not play a huge role in adding to uncertainty. Indeed, snowpack characteristics were computed directly from the daily time series of SWE, and individual values were not often mathematically manipulated. For example, peak SWE date picks were made directly from the data, and thus were only subject to the precision of the instrument, $\pm$ 0.1 inches (2.54 mm).

The air temperature data did not play a large role in the methodology of this work, only in picking the dates of snowmelt onset. Regardless, air temperature was only used qualitatively to gauge when snowmelt onset begins (when temperatures are consistently above 0 ºC).

The other data that were used in this study are USGS streamflow discharge measurements that are made continuously every day at each gauge. The USGS has its own uncertainty procedure for daily mean discharge data, and it is as follows. Discharge is not a quantity that is easily directly measured, and thus the USGS uses stage-discharge relationships to estimate discharge. Stage is a quantity that can be directly measured, and is the water level above some arbitrary datum, often the river bed. These stage-discharge relationships are relatively predictable, unless the morphology of the riverbed or channel change often. If that is the case, then daily mean discharges are computed "by the shifting-control method in which correction factors that are based on individual discharge measurements… are used when applying the gauge heights to the rating tables" (USGS Annual Water Data Report Documentation, 2024). The final daily mean discharge values are reported by the USGS with uncertainties that scale with the magnitude of the discharge measurement. These uncertainties are summarized in **Table 2**.

Discharge (cubic feet per second)	USGS Reported Uncertainty
< 1	Nearest 0.01 cubic feet per second
1.0 – 10	Nearest 0.1 cubic feet per second
10 to 1000	Nearest whole number
> 1000	3 significant figures

Table 2 USGS Reported mean daily discharge uncertainties. Number of significant digits depends on the magnitude of the discharge that is measured. Larger discharges have smaller larger uncertainties.

Although there is inherent uncertainty in the mean daily discharge data, they are precise enough for the purposes of this study, namely in picking dates and durations from the data rather than looking at precise day-to-day magnitudes. Any channel variability that could have influenced the mean daily discharge measurements was assumed to be negligible. In the next section, the uncertainty in these picked characteristics will be discussed, but to address any potential outliers or noise in the data collection, a 3-day running mean was computed on both the SWE and discharge data to smooth them for later analyses.

6.2 Uncertainty in Computed/Picked Characteristics

The characteristic time series that were computed/picked as mentioned in Section 3.0 were subject to not only the measurement uncertainty at the SNOTEL stations and USGS gauges, but also to the definition of the characteristic in question. This proved most true for the date of snowmelt onset, derived from daily SWE and air temperature time series, as well as smoothed discharge hydrographs. The date of snowmelt was the most important characteristic in this study as it was the baseline for subsequent streamflow characteristics, and grounded the snowpack-streamflow comparisons in a reliable reference point.

The date of snowmelt proved more difficult to pick because it was particularly susceptible to oddities and inconsistencies in the smoothed hydrographs. The tedious process of picking the snowmelt onset dates was continually tested by mid-winter rainstorms and resultant peaks in streamflow that clouded the true snowmelt onset date. Moreover, there were also years in certain locations (particularly the American Southwest, HUC15) that had much smaller amounts of snow and thus were susceptible to quick melts and repeated deposition of snows that resulted in multiple apparent snowmelt onsets. See Section 10.2 for a more in-depth description of the process of picking snowmelt onsets.

6.3 Other Factors

Aside from the uncertainty in computing and making picks of characteristics, this study had some limitations that could be addressed in future work. In keeping with the difficulties that were experienced in picking the snowmelt onset dates, the fact that many of the watersheds span large elevation ranges potentially had an impact. More specifically, the date of snowmelt onset picks were based on the response at the stream gauge, the outflow point of the watershed. Streamflow is an integrated response from a watershed, meaning that melt initiation within each watershed can be much more heterogeneous. As some of the watersheds span hundreds or thousands of meters elevation, temperature and other melt-related parameters vary broadly too. Consequently, snowmelt onset picks may not be representative of the snow that fell at the SNOTEL station melting, and rather may be related to snow at lower elevations.

Similarly, the streamflow hydrographs were potentially susceptible to rain-event perturbations of the snowmelt response when the watershed spanned wide swaths of elevation because that straddled the snow-rain line. As a result, precipitation from the same storm could be falling as snow at the high-elevation SNOTEL station but also as rain or sleet near the USGS stream gauge. I suspect that this could be a main reason that many of the streamflow hydrographs had large peaks even when the recorded temperature at the SNOTEL station was well below 0°C. Winter rainfall events are becoming more common in snow-dominated regions, so this is likely to become a greater problem in the future (Knowles et al., 2006).

7.0 Future Work

This current study approached hydrologic data on a year-by-year basis for 121 high-elevation SNOTEL stations and their accompanying 69 small watersheds. Although this work focused firstly on addressing the April 1 SWE estimate, there can be more done in this area to address its farther-reaching impacts on streamflow. Specifically, more work must be done to investigate how snowpack is changing, and how the April 1 assumption has been and will continue to influence our understanding of diminishing snowpacks within the context of the warming climate.

A key limitation of this study is its focus on purely high-elevation snowpacks. The 2500-meter elevation threshold was applied in order to remove the influence of rain-on-snow events and increase the likelihood that the system in question was as snow dominated as possible. Despite that, the Mann-Kendall results could be interpreted to suggest that some snowpacks are moving off the map, meaning that they have too little snowpack to quantify changing trends. This is supported by other studies, particularly on the topic of changing snow/rain ratios at low elevations. More work must be done in this area, particularly to get a sense of which locations are transitioning to rain-dominated from being traditionally snow-dominated. Similarly, work in quantifying changing precipitation ratios at high elevations are needed in order to accurately represent the trends in snowpack patterns across wide spatial scales.

In a similar vein, the elevation threshold served to eliminate subpar streamflow hydrographs: curves that are filled with jagged peaks in the winter even when the temperature is below 0°C. Despite that, snowmelt onset picks proved difficult because a number of such streamflow hydrographs remained. Future work should be done in improving the method of selecting snowmelt onset picks, particularly because it was such a time-intensive part of this work.

Next, it would be prudent for future work to establish a more effective set of criteria for handling watersheds that span huge ranges of elevation. It was established in this current study that several potential sources of uncertainty were introduced by considering such watersheds, and future work would do well to address this. Looking at purely small watersheds that are entirely located at high elevations would be an appropriate step to take.

Lastly, and perhaps most importantly, more work is needed in assessing how the April 1 assumption carries into the calculation and understanding of streamflow trends in this region. This study found that the April 1 assumption did play a role in snowpack characteristics, but it was out of the scope of the project to fully explore how the April 1 assumption carries on. Moreover, clear relations in streamflow (i.e., rise time vs basin area) that were expected to be seen, were not present in these data.

8.0 Conclusions

The western United States has been the focus of intense water resource and climate change research for the last century at least. In this study, the drivers of high-elevation snowpack and streamflow characteristics in this region were evaluated using a large number of SNOTEL daily snow water equivalent (SWE) records and USGS mean daily discharge measurements from 1980 through 2022. This research challenged a common assumption used in quantifying snow-related change in the American west: that the date of peak snowpack generally occurs on April 1. Statistical tests were implemented to determine that at high elevations (> 2000 meters), the April 1 assumption was not accurate, and consequently altered interpretation of snowpack trends.

Drivers of variable snowmelt flow were also investigated, with results indicating that latitude and basin morphology play an important role in the onset of snowmelt, the magnitude of snowmelt flows, and the subsequent availability of surficial waters in stream channels. Generally, northerly locations see more intense snowpacks and snowmelts, while the American Southwest is particularly susceptible to weak snowpacks.

The results of this study provided a fresh perspective for past and future studies of snowpack change in this region, and globally, showing that when data are available, it is imperative to compute the true date of peak snowpack. Climate change has been shown to alter the way snowpacks develop, and it will continue to in the future as well. While this study focused on solely high-elevation snowpacks, the snowmelt analysis was subject to lower elevation processes. Future work can be done with lower elevation snowpacks. This work expanded the literature regarding what drives the various characteristics of snowpack and snowmelt in what is already a water-needy region. Studies such as this, and others, only further add to the knowledge that is necessary to improve water-resource management and sub-seasonal planning of water resources. These results are not only applicable to the North American snowpacks, but challenging the April 1 assumption sets an important precedent for future studies in regions dependent on snowmelt world-wide.

9.0 Acknowledgements

I would like to sincerely thank my advisor, Dr. Karen Prestegaard, for her continued support and advice throughout this project. She did not hesitate to push me and encourage me to develop my own intuition and drive for answering the scientific questions we had identified. Moreover, I would like to thank Dr. Phil Piccoli for his constant availability and tireless effort to ensure that all of the Senior Thesis students under his care are informed, supported, and challenged to be better. His critiques and edits for my papers were especially helpful and, I believe, made me a significantly better scientific writer and presenter. Lastly, I would like to thank my family and closest friends for their constant support in what has been an incredibly rewarding and challenging experience. My work, my career, and my life are better for it.

UMD Honor Pledge: I pledge on my honor that I have not given or received any unauthorized assistance on this assignment.

-Ethan Heidtman (April 22, 2024)

10.0 References

Bourrel, L., Rau, P., Dewitte, B., Labat, D., Lavado, W., Coutaud, A., Vera, A., Alvarado, A., & Ordoñez, J. (2015). Low-frequency modulation and trend of the relationship between ENSO and precipitation along the northern to centre Peruvian Pacific coast. *Hydrological Processes*, *29*(6), 1252–1266. https://doi.org/10.1002/hyp.10247

Clow, D. W. (2010). Changes in the Timing of Snowmelt and Streamflow in Colorado: A Response to Recent Warming. *Journal of Climate*, *23*(9), 2293–2306. https://doi.org/10.1175/2009JCLI2951.1

De Cicco, L. A., Hirsch, R. M., Lorenz, D., Watkins, W. D., & Johnson, M. (2023). Water / dataRetrieval · GitLab. Retrieved November 9, 2023, from https://code.usgs.gov/water/dataRetrieval

Dierauer, J. R., Whitfield, P. H., & Allen, D. M. (2018). Climate Controls on Runoff and Low Flows in Mountain Catchments of Western North America. *Water Resources Research*, *54*(10), 7495–7510. https://doi.org/10.1029/2018WR023087

Fang, X., & Pomeroy, J. W. (2020). Diagnosis of future changes in hydrology for a Canadian Rocky Mountain headwater basin. *Hydrology and Earth System Sciences*, *24*(5). https://doi.org/10.5194/hess-24-2731-2020

Hammond, J. C., & Kampf, S. K. (2020). Subannual Streamflow Responses to Rainfall and Snowmelt Inputs in Snow-Dominated Watersheds of the Western United States. *Water Resources Research*, *56*(4), e2019WR026132. https://doi.org/10.1029/2019WR026132

Kenney, D. S., Klein, R. A., & Clark, M. P. (2004). Use and Effectiveness of Municipal Water Restrictions During Drought in Colorado1. *JAWRA Journal of the American Water Resources Association*, *40*(1), 77–87. https://doi.org/10.1111/j.1752-1688.2004.tb01011.x

Knowles, N., Dettinger, M. D., & Cayan, D. R. (2006). Trends in Snowfall versus Rainfall in the Western United States. *Journal of Climate*, *19*(18), 4545–4559. https://doi.org/10.1175/JCLI3850.1

Liu, F., Hunsaker, C., & Bales, R. C. (2013). Controls of streamflow generation in small catchments across the snow–rain transition in the Southern Sierra Nevada, California. *Hydrological Processes*, *27*(14), 1959–1972. https://doi.org/10.1002/hyp.9304

López-Moreno, J. I., Revuelto, J., Gilaberte, M., Morán-Tejeda, E., Pons, M., Jover, E., Esteban, P., Garcia, C., & Pomeroy, J.W. (2014). The effect of slope aspect on the response of snowpack to climate warming in the Pyrenees. *Theoretical and Applied Climatology*, *117*(1–2), 207–219.

McCabe, G. J., Wolock, D., & Valentin, M. (2018). Warming is Driving Decreases in Snow Fractions While Runoff Efficiency Remains Mostly Unchanged in Snow-Covered Areas of the Western United States. *Journal of Hydrometeorology*, *19*(5). https://doi.org/10.1175/JHM-D-17-0227.1

McLeod, A.I, (2011). Kendall Rank Correlation and Mann-Kendall Trend Test. R Core Team. Retrieved April 1, 2024, from https://cran.r-project.org/web/packages/Kendall/Kendall.pdf.

Miller, W. P., & Piechota, T. C. (2011). Trends in Western U.S. Snowpack and Related Upper Colorado River Basin Streamflow1. *JAWRA Journal of the American Water Resources Association*, *47*(6), 1197–1210. https://doi.org/10.1111/j.1752-1688.2011.00565.x

Montoya, E. L., Dozier, J., & Meiring, W. (2014). Biases of April 1 snow water equivalent records in the Sierra Nevada and their associations with large-scale climate indices.

Geophysical Research Letters, *41*(16), 5912–5918. https://doi.org/10.1002/2014GL060588

Mote, P. W. (2006). Climate-Driven Variability and Trends in Mountain Snowpack in Western North America. *Journal of Climate*, *19*(23), 6209–6220. https://doi.org/10.1175/JCLI3971.1

Mote, P. W., Li, S., Lettenmaier, D. P., Xiao, M., & Engel, R. (2018). Dramatic declines in snowpack in the western US. *Npj Climate and Atmospheric Science*, *1*(1), 2. https://doi.org/10.1038/s41612-018-0012-1

Mote, P. W., Clark, M., & Hamlet, A. F., (2004). Variability and trends in Mountain Snowpack in Western North America. *Preprints, 15th Symp. on global change and climate variations, Seattle, WA, Amer. Meteor. Soc* (Vol. 5).

R Core Team (2021). R: A language and environment for statistical computing. R Foundation for Statistical Computing, Vienna Austria. Accessed August 1, 2024, from https://www.R-project.org/

Stewart, I. T., Cayan, D. R., & Dettinger, M. D. (2005). Changes toward Earlier Streamflow Timing across Western North America. *Journal of Climate*, *18*(8), 1136–1155. https://doi.org/10.1175/JCLI3321.1

University of Nevada, Reno (2022). Study sheds light on what influences water supplied by snowmelt. Retrieved November 3, 2023, from https://www.unr.edu/nevada-today/news/2022/snowmelt-study

U.S. EPA, O. (2016). Climate Change Indicators: Snowpack [Reports and Assessments]. Retrieved September 24, 2023, from https://www.epa.gov/climate-indicators/climate-change-indicators-snowpack

Water Science School. (2019). Snowmelt Runoff and the Water Cycle. Retrieved September 26, 2023, from https://www.usgs.gov/special-topics/water-science-school/science/snowmelt-runoff-and-water-cycle#

Ye, B., Yang, D., & Kane, D. L. (2003). Changes in Lena River streamflow hydrology: Human impacts versus natural variations. *Water Resources Research*, *39*(7). https://doi.org/10.1029/2003WR001991

11.0 Appendix

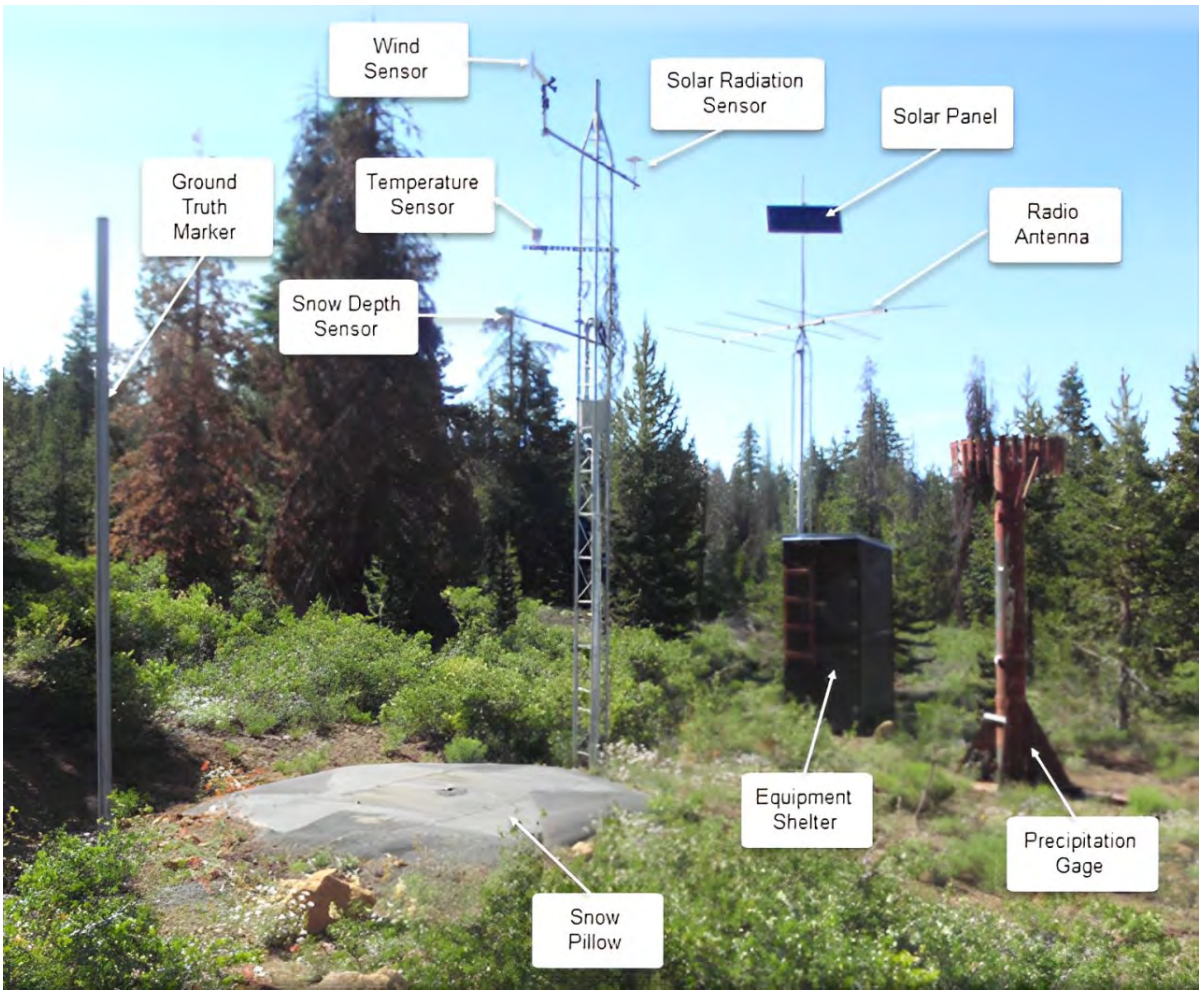

Appendix 1 Sample SNOTEL station. Note the snow pillow in the bottom left of the photo and the shielded thermistor temperature sensor near the top of the tower.

11.1 SNOTEL Data Collection Instructions

These data are collected from the U.S. Department of Agriculture National Water and Climate Center's Snow Telemetry Network (SNOTEL), via the USDA's Report Generator Website: https://wcc.sc.egov.usda.gov/reportGenerator/

To collect these data, select 'Advanced Search', then the SNOTEL network. Do not select a parameter from this advanced search menu. At the time of writing this, there are 897 active SNOTEL sensors. First, select 'Search', and from there the next step is to exit out of this menu and move to the 'Select Columns' panel. Under the 'Data' tab, select snow water equivalent, making sure the 'Value' option is selected, as well as 'None' under function. Then select 'Add' to begin building your report as a CSV file. In the next panel, input dates as 'YYYY-MM-DD' and select output as 'Time Series' and CSV. The report will be generated as a CSV file that can then be put into a text editor and imported into RStudio with the function read.csv().

11.2 Snowmelt Onset Date Picking Procedure

To account for the wide array of variations and difficulties, a number of steps were followed in viewing the four-panel plot that was produced for each station in each year (see Figure 6). First, I examined the streamflow hydrograph, looking for a readily apparent snowmelt onset. If I suspected one, I would confirm its validity by checking first the air temperature reading: did the air temperature at the very least crest 0 °C for a few days? Next, I would see whether this suspected peak begins considerably before the date of peak snowpack, close to the date of peak snowpack, or shortly after. If either of the latter two were true, then I made a pick of the date of snowmelt onset by determining when the streamflow hydrograph departed substantially from a long-term average, the baseflow condition. If there were any other issues and a date of snowmelt onset could not be confidently picked, then 'NA' was input as the date of snowmelt onset for that year. Removing streamflow gauges that were often unintelligible from the data for this study was considered, but it was judged to be worth taking each location on a year-by-year basis to minimize the gaps in the characteristic time series that were produced.

Included at the very end of this document are a few more examples of the four-panel plots that were produced, including some that were too difficult to pick. Each of them is from a HUC8 in a unique large watershed (HUC2) for the water year 2020. The second is an example of one that was declared NA.

11.3 R Scripts

All code written for this project by me, Ethan Heidtman, can be found at the following GitHub link: https://github.com/TroposphericOzone/UMD-Geology-Senior-Thesis-2024-

11.4 SNOTEL Station and USGS Stream Gauge Metadata

Displayed below are the metadata (station information) for first the 207 SNOTEL stations that remained after the implementation of the 2000-meter elevation threshold. The 2500-meter elevation threshold was applied to these stations to further filter the data, leaving 121 stations. Second, the 99 USGS streamflow gauge metadata. The same applies where the 99 shown here are after the application of the 2000-meter elevation threshold and the 69 can be selected after the 2500-meter threshold. For these USGS gauges, the drainage areas are also included in units of square kilometers. Elevations for both the SNOTEL stations and the USGS gauges are reported in meters.

	StationName	StationId	StateName	Elevation	Latitude	Longitude	HUC8	HUC2
1	Badger Pass	307	MONTANA	2103.02	48.13088	-113.02317	10030201	10
2	Baker Butte	308	ARIZONA	2244.13	34.45654	-111.40651	15060203	15
3	Bald Mtn.	309	WYOMING	2858.88	44.8007	-107.84442	10080010	10
4	Baldy	310	ARIZONA	2810.42	33.97845	-109.50357	15020001	15
5	Banner Summit	312	IDAHO	2145.69	44.30342	-115.23447	17050120	17
6	Barker Lakes	313	MONTANA	2514.48	46.09713	-113.13038	17010201	17
7	Base Camp	314	WYOMING	2151.78	43.94019	-110.44544	17040101	17
8	Basin Creek	315	MONTANA	2188.36	45.79737	-112.52047	17010201	17
9	Bateman	316	NEW MEXICO	2818.96	36.51174	-106.31543	13020102	13
10	Bear Canyon	320	IDAHO	2407.8	43.74367	-113.93797	17040218	17
11	Bear Creek	321	NEVADA	2450.47	41.83384	-115.45278	17050102	17
12	Bear Trap Meadow	325	WYOMING	2499.24	43.88743	-107.06135	10090201	10
13	Beartooth Lake	326	WYOMING	2852.79	44.94307	-109.56743	10070006	10
14	Beaver Dams	329	UTAH	2435.23	39.13683	-111.55813	16030004	16
15	Beaver Divide	330	UTAH	2523.62	40.61233	-111.09782	16020203	16
16	Ben Lomond Peak	332	UTAH	2343.49	41.37603	-111.94405	16020102	16
17	Berry Creek	334	NEVADA	2857.97	39.31917	-114.62278	16060008	16
18	Berthoud Summit	335	COLORADO	3448.34	39.80364	-105.77786	14010001	14
19	Big Bend	336	NEVADA	2102.41	41.76168	-115.6931	17050104	17
20	Big Flat	339	UTAH	3154.22	38.30183	-112.35672	16030007	16
21	Black Flat-U.M. Ck	348	UTAH	2869.25	38.6799	-111.59765	14070003	14
22	Black Pine	349	MONTANA	2197.5	46.414	-113.43095	17010202	17
23	Blind Bull Sum	353	WYOMING	2636.39	42.964	-110.60973	14040101	14
24	Blue Lakes	356	CALIFORNIA	2458.7	38.60801	-119.92455	18040012	18
25	Bone Springs Div	358	WYOMING	2849.74	44.67888	-107.5811	10080010	10
26	Bostetter R.S.	359	IDAHO	2285.89	42.16442	-114.19272	17040212	17
27	Box Canyon	363	MONTANA	2032.92	45.2719	-110.24903	10070002	10
28	Box Creek	364	UTAH	3003.05	38.50809	-112.01856	16030002	16
29	Brown Duck	368	UTAH	3222.8	40.58102	-110.58587	14060003	14
30	Buck Flat	371	UTAH	2867.72	39.134	-111.43722	14060009	14
31	Buckskin Lower	373	NEVADA	2112.16	41.75067	-117.53182	16040109	16
32	Bug Lake	374	UTAH	2434.32	41.68541	-111.41987	16010201	16
33	Burgess Junction	377	WYOMING	2401.71	44.78765	-107.52917	10090101	10
34	Burro Mountain	378	COLORADO	2839.68	39.87504	-107.59902	14050005	14
35	Burroughs Creek	379	WYOMING	2666.87	43.69733	-109.67021	10080001	10
36	Butte	380	COLORADO	3108.81	38.89435	-106.95327	14020001	14
37	Carrot Basin	385	MONTANA	2743.07	44.96192	-111.29403	10020008	10
38	Castle Valley	390	UTAH	2928.07	37.66098	-112.74093	16030001	16
39	Cedar Pass	391	CALIFORNIA	2142.64	41.58233	-120.3025	18020002	18
40	Chalk Creek #1	392	UTAH	2795.18	40.85464	-111.04765	16020101	16
41	Chalk Creek #2	393	UTAH	2501.68	40.88529	-111.06954	16020101	16
42	Chamita	394	NEW MEXICO	2555.01	36.95606	-106.65723	13020102	13
43	Chepeta	396	UTAH	3199.94	40.77458	-110.0105	14060003	14
44	Clear Creek #1	399	UTAH	2735.45	39.86671	-111.28363	16020202	16
45	Clear Creek #2	400	UTAH	2388.6	39.89275	-111.25154	16020202	16
46	Cole Creek	407	MONTANA	2392.56	45.19405	-109.34548	10070006	10
47	Columbine	408	COLORADO	2793.97	40.39591	-106.60437	10180001	10
48	Copper Camp	414	MONTANA	2118.26	47.08158	-112.72955	17010203	17
49	Copper Mountain	415	COLORADO	3207.25	39.48917	-106.17154	14010002	14
50	Coronado Trail	416	ARIZONA	2565.68	33.80418	-109.15352	15040004	15
51	Culebra #2	430	COLORADO	3219.14	37.20939	-105.19988	13010002	13
52	Cumbres Trestle	431	COLORADO	3058.52	37.01877	-106.45275	13020102	13
53	Currant Creek	432	UTAH	2412.37	40.35747	-111.08993	14060004	14
54	Daniels-Strawberry	435	UTAH	2440.72	40.2953	-111.25677	14060004	14
55	Darkhorse Lake	436	MONTANA	2726.3	45.17367	-113.58448	10020004	10

56	Deadwood Summit	439	IDAHO	2090.83	44.54514	-115.5638	17050120	17
57	Dills Camp	444	UTAH	2812.56	39.04554	-111.46875	14070002	14
58	Divide	448	MONTANA	2377.32	44.79317	-112.05645	10020003	10
59	Divide Peak	449	WYOMING	2660.77	41.30399	-107.15255	14050003	14
60	Dollarhide Summit	450	IDAHO	2566.29	43.6025	-114.67417	17040219	17
61	Dome Lake	451	WYOMING	2706.49	44.57462	-107.29537	10090101	10
62	Dorsey Basin	453	NEVADA	2408.72	40.89343	-115.21104	16040101	16
63	Dry Lake	457	COLORADO	2520.88	40.5337	-106.7814	14050001	14
64	Ebbetts Pass	462	CALIFORNIA	2639.74	38.5497	-119.80468	16050201	16
65	Echo Peak	463	CALIFORNIA	2332.52	38.849	-120.0795	16050101	16
66	Elk River	467	COLORADO	2663.52	40.84758	-106.96861	14050001	14
67	Elkhart Park G.S.	468	WYOMING	2864.98	43.00657	-109.75893	14040102	14
68	Farmington	474	UTAH	2408.41	40.97462	-111.80975	16020102	16
69	Farnsworth Lake	475	UTAH	2932.95	38.77246	-111.67662	16030003	16
70	Fawn Creek	476	NEVADA	2142.94	41.82098	-116.10153	17050104	17
71	Fish Creek	477	OREGON	2334.65	42.70992	-118.6321	17120003	17
72	Fisher Creek	480	MONTANA	2773.54	45.06235	-109.94488	10070006	10
73	Five Points Lake	481	UTAH	3335.26	40.71785	-110.46721	14060003	14
74	Fremont Pass	485	COLORADO	3452	39.38014	-106.19784	14010002	14
75	Frisco Divide	486	NEW MEXICO	2442.24	33.73687	-108.94327	15040004	15
76	Fry	488	ARIZONA	2205.43	35.07356	-111.84477	15060202	15
77	Gallegos Peak	491	NEW MEXICO	2889.36	36.19418	-105.55742	13020101	13
78	Giveout	493	IDAHO	2112.16	42.4132	-111.1663	16010201	16
79	Gooseberry RS	495	UTAH	2421.21	38.80034	-111.68333	16030003	16
80	Granite Peak	498	NEVADA	2591.59	41.67032	-117.56668	16040109	16
81	Grassy Lake	499	WYOMING	2214.26	44.12612	-110.83435	17040203	17
82	Grizzly Peak	505	COLORADO	3395	39.64646	-105.8694	14010002	14
83	Hagans Meadow	508	CALIFORNIA	2359.65	38.8519	-119.9374	16050101	16
84	Hannagan Meadows	511	ARIZONA	2751.3	33.65352	-109.30877	15060101	15
85	Harris Flat	514	UTAH	2374.89	37.48997	-112.57602	16030001	16
86	Hayden Fork	517	UTAH	2782.69	40.79669	-110.88472	16010101	16
87	Heavenly Valley	518	CALIFORNIA	2601.04	38.92431	-119.91641	16050101	16
88	Hopewell	532	NEW MEXICO	3076.81	36.71632	-106.2637	13020102	13
89	Horse Ridge	533	UTAH	2498.93	41.31372	-111.44624	16020101	16
90	Howell Canyon	534	IDAHO	2432.19	42.32029	-113.61587	17040209	17
91	Hyndman	537	IDAHO	2322.46	43.71077	-114.15894	17040219	17
92	Idarado	538	COLORADO	2990.55	37.93389	-107.6762	14020006	14
93	Independence Camp	539	CALIFORNIA	2127.4	39.45269	-120.29367	16050102	16
94	Independence Lake	541	CALIFORNIA	2541.3	39.42752	-120.31342	16050102	16
95	Independence Pass	542	COLORADO	3230.11	39.07543	-106.61154	14010004	14
96	Indian Creek	544	WYOMING	2872.6	42.30023	-110.67753	14040107	14
97	Jackson Peak	550	IDAHO	2154.83	44.05092	-115.44322	17050120	17
98	Kelley R.S.	554	WYOMING	2493.14	42.26554	-110.80177	14040107	14
99	Kiln	556	COLORADO	2933.25	39.3172	-106.61501	14010004	14
100	Kimberly Mine	557	UTAH	2773.85	38.48383	-112.39273	16030003	16
101	Kolob	561	UTAH	2823.22	37.52664	-113.05386	15010008	15
102	Lake Irene	565	COLORADO	3255.71	40.41446	-105.81941	14010001	14
103	Lakefork #1	566	UTAH	3086.86	40.59709	-110.43316	14060003	14
104	Lamoille #3	570	NEVADA	2453.83	40.6448	-115.3812	16040101	16
105	Lasal Mountain	572	UTAH	2919.23	38.48226	-109.27198	14030005	14
106	Laurel Draw	573	NEVADA	2036.57	41.77637	-116.02957	17050104	17
107	Leavitt Meadows	575	CALIFORNIA	2193.84	38.30367	-119.55111	16050302	16
108	Lewis Lake Divide	577	WYOMING	2392.56	44.20862	-110.66628	17040101	17
109	Lick Creek	578	MONTANA	2090.83	45.5041	-110.96625	10020008	10
110	Lily Lake	579	UTAH	2783.6	40.86493	-110.79813	16010101	16

111	Lily Pond	580	COLORADO	3373.67	37.38028	-106.54823	13010002	13
112	Little Warm	585	WYOMING	2855.84	43.50278	-109.752	10080001	10
113	Lizard Head Pass	586	COLORADO	3106.67	37.79895	-107.92475	14030002	14
114	Lobdell Lake	587	CALIFORNIA	2818.96	38.43745	-119.36572	16050302	16
115	Lone Cone	589	COLORADO	2973.18	37.89169	-108.19636	14030003	14
116	Long Flat	592	UTAH	2432.79	37.51255	-113.39661	16030006	16
117	Lookout Mountain	595	NEW MEXICO	2593.42	33.36089	-107.83203	15040001	15
118	Loomis Park	597	WYOMING	2511.43	43.17387	-110.14007	14040101	14
119	Lost-Wood Divide	601	IDAHO	2407.8	43.82432	-114.26402	17040219	17
120	Lynx Pass	607	COLORADO	2718.38	40.07832	-106.67095	14010001	14
121	Magic Mountain	610	IDAHO	2096.92	42.18072	-114.28662	17040212	17
122	Mammoth-Cottonwood	612	UTAH	2654.37	39.68338	-111.31818	16030004	16
123	Marlette Lake	615	NEVADA	2402.93	39.16395	-119.89672	16050101	16
124	Marquette	616	WYOMING	2669.92	44.3016	-109.24019	10080013	10
125	Maverick Fork	617	ARIZONA	2810.12	33.92123	-109.45872	15060101	15
126	Mc Clure Pass	618	COLORADO	2674.18	39.12899	-107.28834	14020004	14
127	Merchant Valley	621	UTAH	2653.15	38.30285	-112.43637	16030007	16
128	Middle Creek	624	COLORADO	3434.62	37.61779	-107.03932	13010001	13
129	Midway Valley	626	UTAH	2995.12	37.56933	-112.83849	16030001	16
130	Mineral Creek	629	COLORADO	3061.87	37.84737	-107.72657	14080104	14
131	Monument Peak	635	MONTANA	2697.35	45.21759	-110.237	10070002	10
132	Morgan Creek	639	IDAHO	2316.37	44.84237	-114.26871	17060203	17
133	Mt Rose Ski Area	652	NEVADA	2682.41	39.31573	-119.89473	16050102	16
134	Mule Creek	656	MONTANA	2529.72	45.40957	-112.95927	10020004	10
135	North Costilla	665	NEW MEXICO	3230.11	36.99396	-105.25988	13020101	13
136	North French Creek	668	WYOMING	3094.48	41.33087	-106.37558	10180002	10
137	Palisades Tahoe	784	CALIFORNIA	2442.24	39.18986	-120.26576	16050102	16
138	Park Cone	680	COLORADO	2932.34	38.81982	-106.58962	14020001	14
139	Park Reservoir	682	COLORADO	3043.89	39.04433	-107.87951	14020005	14
140	Parleys Summit	684	UTAH	2311.8	40.76184	-111.62917	16020102	16
141	Payson R.S.	686	UTAH	2451.69	39.92976	-111.63109	16020202	16
142	Peterson Meadows	930	MONTANA	2194.45	46.12588	-113.30792	17010202	17
143	Phantom Valley	688	COLORADO	2756.78	40.39803	-105.84606	14010001	14
144	Phillips Bench	689	WYOMING	2499.24	43.51687	-110.91258	17040103	17
145	Pickle Keg	691	UTAH	2749.16	39.01219	-111.58259	16030003	16
146	Placer Basin	696	MONTANA	2691.25	45.41905	-110.08844	10070002	10
147	Poison Flat	697	CALIFORNIA	2357.82	38.50576	-119.62624	16050201	16
148	Pole Creek R.S.	698	NEVADA	2548	41.87255	-115.24713	17050102	17
149	Porphyry Creek	701	COLORADO	3288.02	38.48864	-106.33967	14020003	14
150	Quemazon	708	NEW MEXICO	2897.59	35.92195	-106.39179	13020101	13
151	Red Mountain Pass	713	COLORADO	3377.02	37.89168	-107.71389	14080104	14
152	Red Pine Ridge	714	UTAH	2739.41	39.45197	-111.27221	14060009	14
153	Red River Pass #2	715	NEW MEXICO	3003.66	36.69935	-105.34145	13020101	13
154	Rock Creek	720	UTAH	2403.54	40.54875	-110.69292	14060003	14
155	Rocky Basin-Settleme	723	UTAH	2652.85	40.44293	-112.22377	16020304	16
156	Rubicon #2	724	CALIFORNIA	2322.16	38.99927	-120.13139	16050101	16
157	S Fork Shields	725	MONTANA	2468.76	46.0896	-110.43363	10070003	10
158	Saddle Mtn.	727	MONTANA	2419.99	45.69259	-113.96828	17010205	17
159	Salt River Summit	730	WYOMING	2328.56	42.5075	-110.9099	17040105	17
160	Seeley Creek	742	UTAH	3018.59	39.31042	-111.43297	14060009	14
161	Senorita Divide #2	744	NEW MEXICO	2611.7	36.00152	-106.83408	13020202	13
162	Seventysix Creek	746	NEVADA	2240.17	41.73732	-115.47215	17050102	17
163	Shell Creek	751	WYOMING	2919.84	44.50012	-107.42947	10080010	10
164	Shower Falls	754	MONTANA	2468.76	45.40125	-110.95758	10020008	10

165	Signal Peak	755	NEW MEXICO	2561.72	32.92342	-108.14546	15040001	15
166	Silver Creek Divide	757	NEW MEXICO	2772.33	33.3696	-108.70711	15040004	15
167	Silvies	759	OREGON	2130.45	42.75333	-118.68785	17120003	17
168	Skalkaho Summit	760	MONTANA	2209.69	46.24212	-113.7725	17010202	17
169	Slug Creek Divide	761	IDAHO	2202.07	42.56248	-111.29797	17040207	17
170	Slumgullion	762	COLORADO	3523.32	37.99076	-107.20392	14020002	14
171	Smith Morehouse	763	UTAH	2325.82	40.78931	-111.09192	16020101	16
172	Snider Basin	765	WYOMING	2456.57	42.4949	-110.53203	14040101	14
173	Somsen Ranch	770	IDAHO	2072.54	42.95275	-111.35933	17040207	17
174	Sonora Pass	771	CALIFORNIA	2672.97	38.31021	-119.6003	16050302	16
175	South Brush Creek	772	WYOMING	2589.15	41.3295	-106.5025	10180002	10
176	Spring Creek Divide	779	WYOMING	2743.07	42.52516	-110.66148	14040101	14
177	Steel Creek Park	790	UTAH	3096.01	40.90862	-110.50462	14040107	14
178	Stickney Mill	792	IDAHO	2264.55	43.86117	-114.20902	17040218	17
179	Strawberry Divide	795	UTAH	2475.77	40.16483	-111.20665	14060004	14
180	Sucker Creek	798	WYOMING	2706.49	44.7225	-107.40033	10090101	10
181	Summer Rim	800	OREGON	2157.88	42.6957	-120.80158	18010202	18
182	Summit Ranch	802	COLORADO	2856.14	39.71803	-106.1577	14010002	14
183	Swede Peak	805	IDAHO	2328.56	43.626	-113.96887	17040221	17
184	Tahoe City Cross	809	CALIFORNIA	2071.62	39.17162	-120.15362	16050101	16
185	Togwotee Pass	822	WYOMING	2919.84	43.74902	-110.0578	10080001	10
186	Tower	825	COLORADO	3236.82	40.5374	-106.67655	14050001	14
187	Trial Lake	828	UTAH	3045.41	40.678	-110.94873	16020203	16
188	Two Ocean Plateau	837	WYOMING	2816.21	44.15178	-110.22122	17040101	17
189	Upper San Juan	840	COLORADO	3090.52	37.48563	-106.83528	14080101	14
190	Vail Mountain	842	COLORADO	3142.33	39.61765	-106.38019	14010003	14
191	Vernon Creek	844	UTAH	2255.71	39.93667	-112.41478	16020304	16
192	Virginia Lakes Ridge	846	CALIFORNIA	2864.98	38.07298	-119.23433	16050301	16
193	Ward Creek #3	848	CALIFORNIA	2055.78	39.13545	-120.21865	16050101	16
194	Warm Springs	850	MONTANA	2377.32	46.27368	-113.164	17010201	17
195	Webber Springs	852	WYOMING	2822.31	41.1591	-106.92809	10180002	10
196	Webster Flat	853	UTAH	2804.94	37.575	-112.90155	15010008	15
197	Whiskey Ck	857	COLORADO	3136.24	37.21423	-105.12262	11020010	11
198	White Elephant	860	IDAHO	2349.89	44.53267	-111.41085	17040202	17
199	White Horse Lake	861	ARIZONA	2195.37	35.14189	-112.14966	15060202	15
200	White Mill	862	MONTANA	2651.63	45.04575	-109.90987	10070006	10
201	White River #1	864	UTAH	2633.65	39.9645	-110.98845	14060007	14
202	Widtsoe #3	865	UTAH	2938.13	37.83633	-111.88163	16030002	16
203	Wilbur Bench	543	UTAH	2795.18	39.89166	-110.74604	14060004	14
204	Willow Creek	868	WYOMING	2462.66	42.81513	-110.83515	17040105	17
205	Willow Creek Pass	869	COLORADO	2902.47	40.34734	-106.0952	14010001	14
206	Wolverine	875	WYOMING	2331.61	44.80417	-109.657	10070006	10
207	Workman Creek	877	ARIZONA	2143.25	33.81259	-110.91852	15060103	15

	Station	Latitude	Longitude	Elevation	HUC	HUC2	Drainage
1	11348500	41.40600116	-120.9277458	1301.5	18020002	18	3709.2
2	10189000	38.19636955	-112.1477005	1877.3	16030002	16	3128.6
3	9024000	39.89998695	-105.7766741	2716	14010001	14	71.5
4	6093200	48.36945	-112.8017806	1261.8	10030201	10	396.6
5	9510000	33.80837509	-111.6634729	478.6	15060203	15	15969.4
6	6279500	44.75856618	-108.1814972	1115.5	10080010	10	40855.4
7	9384000	34.31448635	-109.362315	1831.8	15020001	15	1830
8	13236500	44.29194444	-115.6419444	1578.9	17050120	17	282.5
9	9504500	34.76446436	-111.8909885	1057.6	15060202	15	920.2
10	12324590	46.5194833	-112.7931722	1324	17010201	17	1073.1
11	13011000	43.85855089	-110.586597	2050.5	17040101	17	2091.8
12	8290000	36.07355556	-106.1116944	1723.1	13020102	13	8149.3
13	9260000	40.54901667	-108.4243222	1732.7	14050003	14	10456.2
14	13127000	43.93916667	-113.6483333	1813.6	17040218	17	2076.2
15	13168500	42.7711111	-115.7202778	792	17050102	17	6962.2
16	9239500	40.4829861	-106.8324306	2040.7	14050001	14	1469.7
17	10011500	40.9652254	-110.8535079	2427.6	16010101	16	445.8
18	6311000	44.02774228	-107.0808955	2493.1	10090201	10	63.5
19	6207500	45.0099111	-109.0653667	1214.9	10070006	10	2986
20	8220000	37.6886111	-106.4598611	2432.3	13010001	13	3421.5
21	9063000	39.50831949	-106.3666948	2637.5	14010003	14	182
22	10215900	39.25912877	-111.579916	1982.8	16030004	16	68.4
23	10155000	40.60166667	-111.3358333	1889.3	16020203	16	596.2
24	9489500	33.47672039	-109.7639775	1744.9	15060101	15	1451.5
25	10141000	41.2782765	-112.0918866	1280.2	16020102	16	5394
26	10244950	39.20153889	-114.689161	2243.5	16060008	16	28.8
27	10172700	39.97939105	-112.3802297	1891.8	16020304	16	64.8
28	13174500	41.68879428	-115.8448067	1864.9	17050104	17	541.7
29	10234500	38.2798	-112.568286	1890.7	16030007	16	235.9
30	6298000	44.8494123	-107.3045253	1237.4	10090101	10	534
31	10337500	39.16629577	-120.1443586	1894.7	16050102	16	1314.2
32	9330000	38.3069248	-111.5187917	2099.4	14070003	14	1946.6
33	9166500	37.47249296	-108.4975908	2115.2	14030002	14	1306.4
34	12332000	46.1845694	-113.5015694	1659.3	17010202	17	313.6
35	6630000	41.87218127	-107.0575465	1950.9	10180002	10	10821.7
36	9223000	42.11088889	-110.7094167	2272.2	14040107	14	331.8
37	9188500	43.0190833	-110.1188611	2276.2	14040101	14	1213.1
38	11323500	38.2261111	-121.0233333	25.2	18040012	18	1609.6
39	13088000	42.52796709	-114.0186386	1238.3	17040212	17	44530.9
40	6191500	45.1121194	-110.7936667	1548	10070002	10	6780.7
41	6195600	45.7383611	-110.4794694	1347.2	10070003	10	2192.8
42	10242000	37.67219924	-113.0346702	1823.5	16030006	16	209.7
43	9295000	40.20023757	-110.0637613	1543.9	14060003	14	6850.7
44	9326500	39.10413724	-111.2165589	1892.7	14060009	14	357.7
45	10329500	41.5346175	-117.4179047	1416.9	16040109	16	454.3

46	10068500	42.4015929	-111.356875	1801.2	16010201	16	9603.4
47	10309000	38.84519444	-119.7060833	1534.9	16050201	16	922.8
48	9304500	40.0335849	-107.8622946	1920.1	14050005	14	1969.9
49	6228000	43.01051478	-108.3767701	1493.9	10080001	10	5985
50	9110000	38.66443715	-106.8453172	2441.6	14020001	14	1233.8
51	6025500	45.52658056	-112.701725	1533.9	10020004	10	6407.5
52	6052500	45.88535556	-111.438286	1245.5	10020008	10	4637.1
53	9361500	37.2791688	-107.8803445	1981.6	14080104	14	1817
54	10183500	38.20609038	-112.2077024	1825.4	16030001	16	2931.6
55	10128500	40.7371721	-111.2479652	2022.9	16020101	16	419.9
56	9085000	39.54666667	-107.3308333	1744.3	14010004	14	3766.2
57	13142500	43.24805556	-114.3566667	1420.8	17040219	17	4175.7
58	10150500	40.0496781	-111.5479705	1484.3	16020202	16	1690
59	6620000	40.93663889	-106.3391944	2380.5	10180001	10	3709.2
60	9152500	38.98331575	-108.4506446	1411.6	14020005	14	20536.6
61	12340000	46.8994111	-113.7563194	1019.4	17010203	17	5928
62	9057500	39.88026354	-106.3339175	2341.6	14010002	14	1547.4
63	9444500	33.05604444	-109.2990167	1048	15040004	15	7169.5
64	9310500	39.77440566	-111.191006	2337.7	14060007	14	155.8
65	13027500	43.0797222	-111.0372222	1731	17040105	17	2148.8
66	11501000	42.58430556	-121.8483333	1280.8	18010202	18	4056.5
67	8251500	37.0786111	-105.7569444	2263.8	13010002	13	19958.6
68	9288000	40.20023128	-110.9076623	2032.9	14060004	14	362.9
69	12344000	45.97205	-114.1412333	1201.5	17010205	17	2721.6
70	9330500	38.99105556	-111.253886	1982.8	14070002	14	272.2
71	6019500	45.1923194	-112.1428167	1645.8	10020003	10	1384.1
72	10322500	40.60741747	-116.2017444	1471.9	16040101	16	13097.5
73	13023000	43.14305556	-110.9769444	1746.1	17040103	17	1161.2
74	11434500	38.83101846	-120.0376835	2255	16050101	16	
75	9205000	42.56716598	-109.930151	2072.5	14040102	14	3188.2
76	10217000	39.1552387	-111.877705	1532.8	16030003	16	12755.3
77	13148500	43.39	-113.9997222	1521.4	17040221	17	803.5
78	10396000	42.7908333	-118.8675	1296.6	17120003	17	518.4
79	8279500	36.20555556	-105.9639722	1764.4	13020101	13	26957
80	9406000	37.2041494	-113.1807789	1065.4	15010008	15	2478
81	8324000	35.6619833	-106.7434389	1713.5	13020202	13	1218.2
82	9180500	38.81054095	-109.2934493	1247.3	14030005	14	62467.7
83	13056500	43.8258333	-111.905	1465.9	17040203	17	7568.7
84	13077000	42.7675	-112.8794444	1293.6	17040209	17	35251.5
85	9147500	38.33143056	-107.779225	1926.2	14020006	14	1161.2
86	13039500	44.5944444	-111.3497222	1966.3	17040202	17	245.2
87	10296500	38.51324495	-119.4498872	1682.4	16050302	16	648
88	9172500	38.03070556	-108.1102889	2164	14030003	14	800.9
89	9430500	33.06150278	-108.5373861	1418.7	15040001	15	4831.5
90	6280300	44.20788889	-109.55525	1889.7	10080013	10	769.8
91	9132500	38.9258228	-107.4342211	1914.1	14020004	14	1360.8
92	13302500	45.1836111	-113.8952778	1193.2	17060203	17	9686.4

93	9119000	38.5211111	-106.9409583	2325.1	14020003	14	2750.1
94	13068500	43.13055556	-112.4766667	1346.8	17040207	17	3356.7
95	9128000	38.52915336	-107.648947	1989	14020002	14	10292.9
96	9342500	37.26552778	-107.011	2148	14080101	14	728.4
97	10293000	38.3276958	-119.2148759	1950.6	16050301	16	930.5
98	7128500	38.0342222	-103.2014167	1182	11020010	11	8919.1
99	9498500	33.6194949	-110.9215037	663.6	15060103	15	11161.2

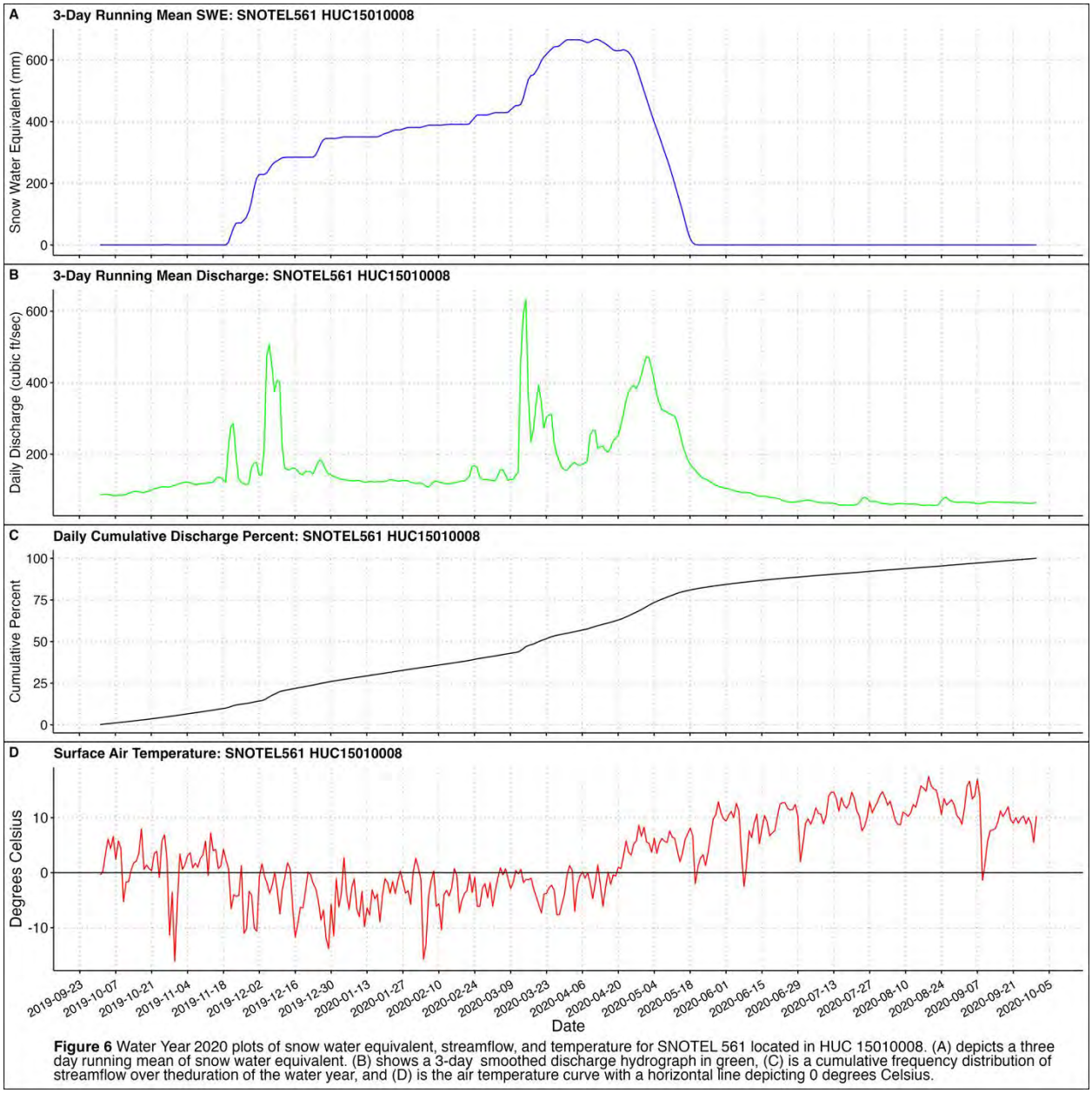

Figure 6 Water Year 2020 plots of snow water equivalent, streamflow, and temperature for SNOTEL 561 located in HUC 15010008. (A) depicts a three day running mean of snow water equivalent. (B) shows a 3-day smoothed discharge hydrograph in green, (C) is a cumulative frequency distribution of streamflow over theduration of the water year, and (D) is the air temperature curve with a horizontal line depicting 0 degrees Celsius.

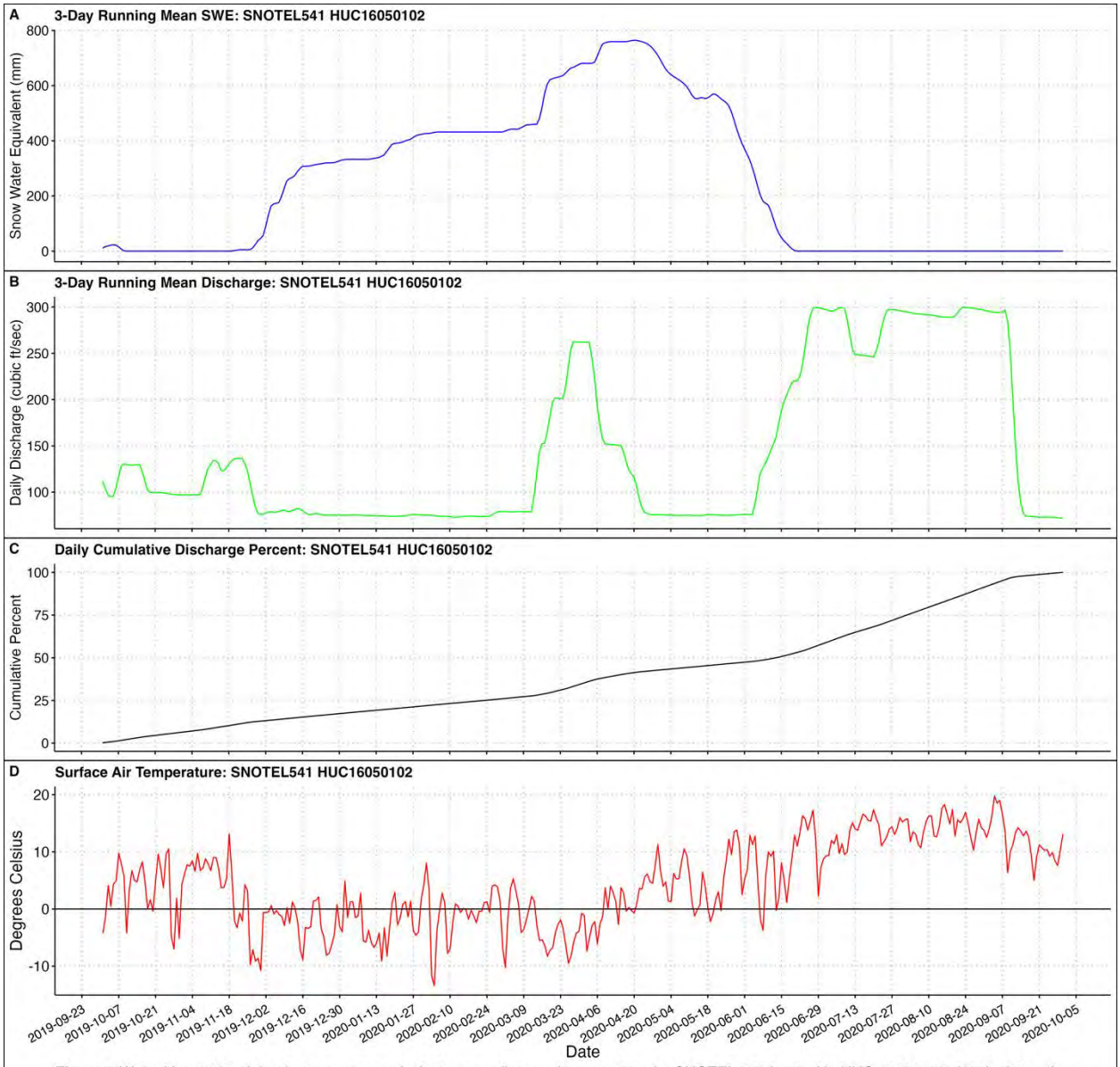

Figure 6 Water Year 2020 plots of snow water equivalent, streamflow, and temperature for SNOTEL 541 located in HUC 16050102. (A) depicts a three day running mean of snow water equivalent. (B) shows a 3-day smoothed discharge hydrograph in green, (C) is a cumulative frequency distribution of streamflow over theduration of the water year, and (D) is the air temperature curve with a horizontal line depicting 0 degrees Celsius.

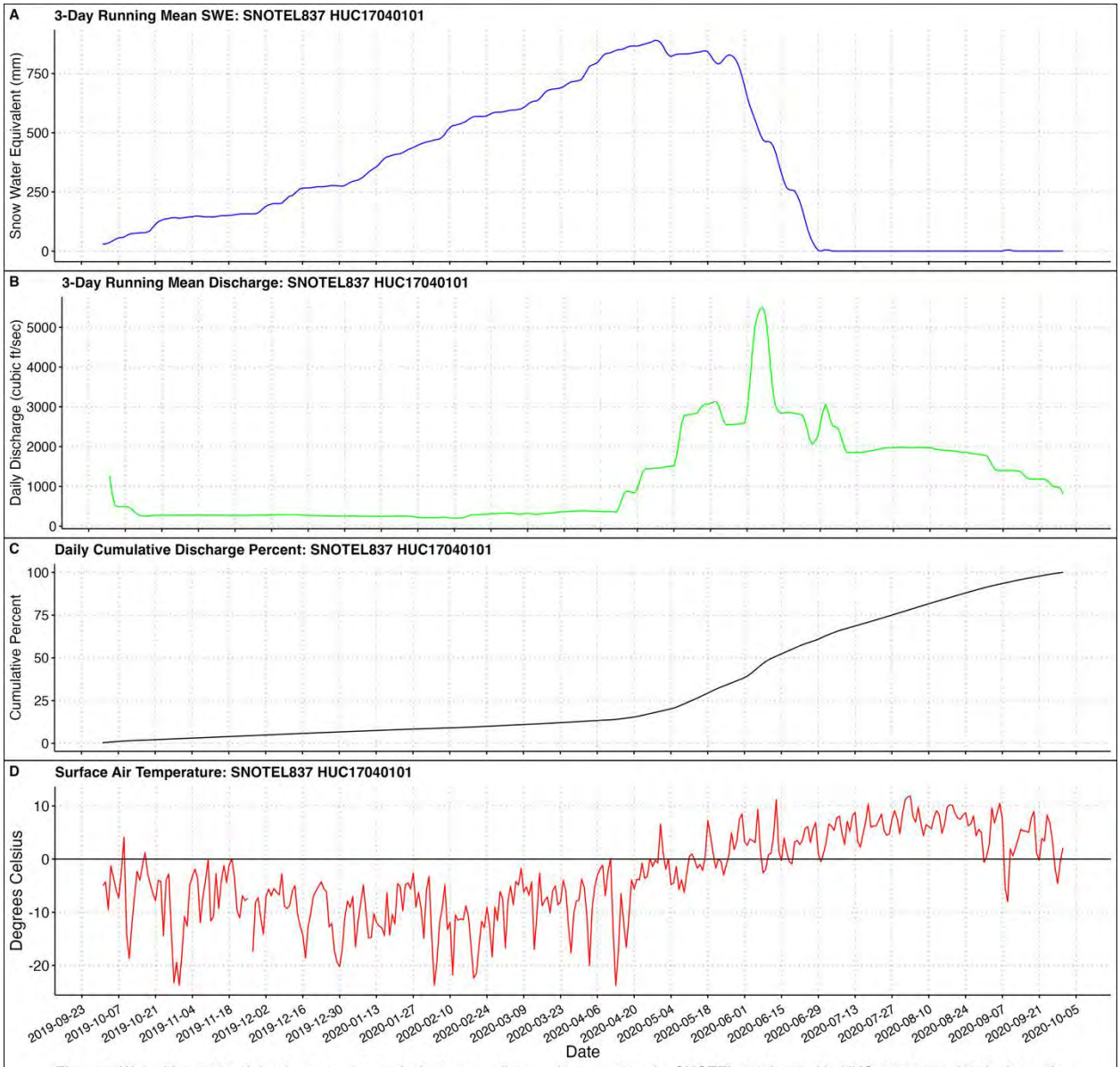

Figure 6 Water Year 2020 plots of snow water equivalent, streamflow, and temperature for SNOTEL 837 located in HUC 17040101. (A) depicts a three day running mean of snow water equivalent. (B) shows a 3-day smoothed discharge hydrograph in green, (C) is a cumulative frequency distribution of streamflow over theduration of the water year, and (D) is the air temperature curve with a horizontal line depicting 0 degrees Celsius.

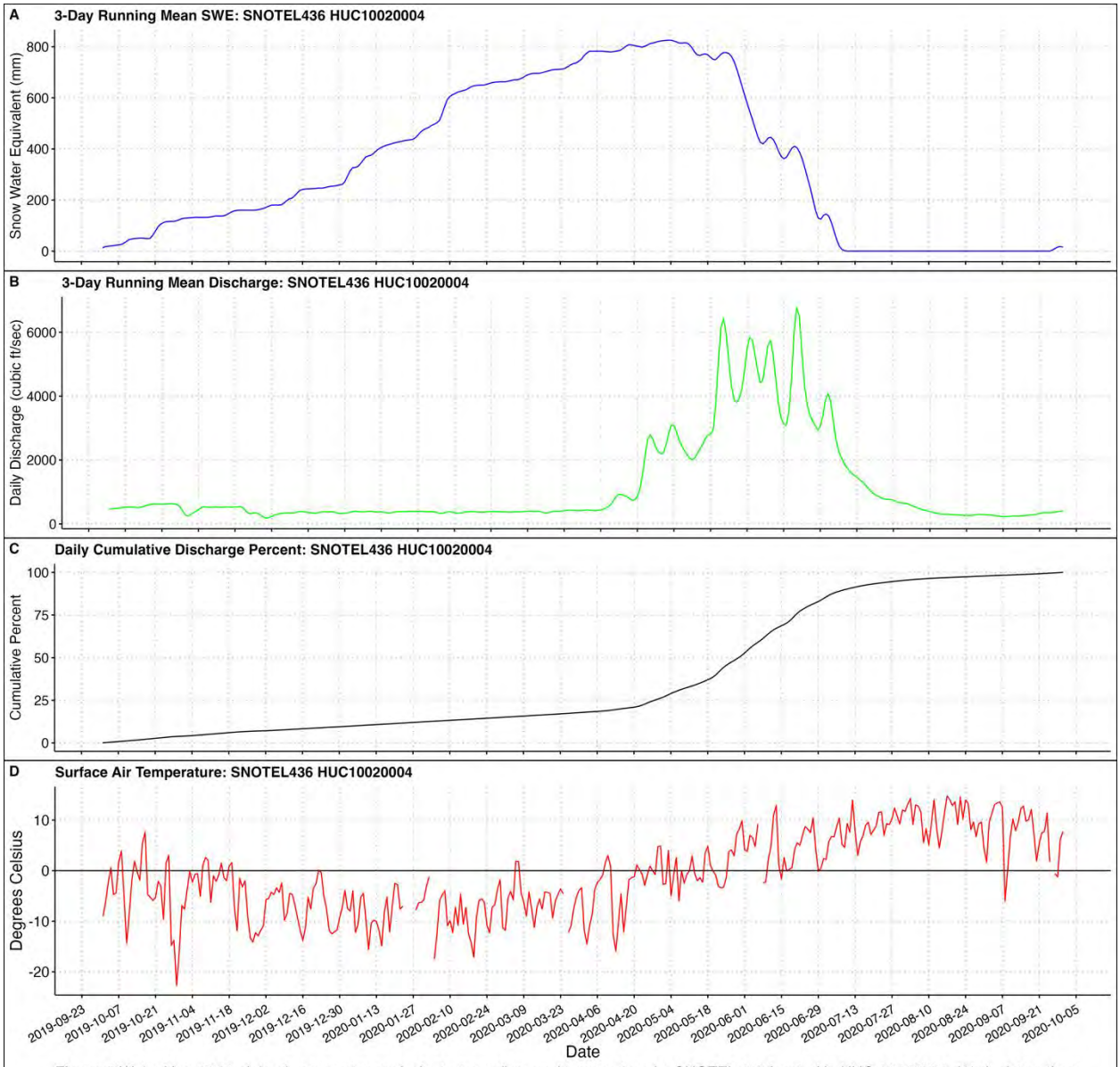

Figure 6 Water Year 2020 plots of snow water equivalent, streamflow, and temperature for SNOTEL 436 located in HUC 10020004. (A) depicts a three day running mean of snow water equivalent. (B) shows a 3-day smoothed discharge hydrograph in green, (C) is a cumulative frequency distribution of streamflow over theduration of the water year, and (D) is the air temperature curve with a horizontal line depicting 0 degrees Celsius.